Tectonophysics 845 (2022) 229643

Contents lists available at ScienceDirect

Tectonophysics

journal homepage: www.elsevier.com/locate/tecto

Seismic anisotropy in the mantle of a tectonically inverted extensional basin: A shear-wave splitting and mantle xenolith study on the western Carpathian-Pannonian region

Nóra Liptai [a,b,*], Zoltán Gráczer [a], Gyöngyvér Szanyi [a], Sierd A.P.L. Cloetingh [b,c], Bálint Süle [a,b], László E. Aradi [a,d], György Falus [e], Götz Bokelmann [f], Máté Timkó [a,b], Gábor Timár [g], Csaba Szabó [b,d], István J. Kovács [a,b], AlpArray Working Group

[a] MTA FI Lendület Pannon LitH$_2$Oscope Research Group, Institute of Earth Physics and Space Science, Sopron, Hungary
[b] Institute of Earth Physics and Space Science, Sopron, Hungary
[c] Tectonics Group, Department of Earth Sciences, Faculty of Geosciences, Utrecht University, Utrecht, Netherlands
[d] Lithosphere Fluid Research Laboratory, Department of Petrology and Geochemistry, Institute of Geography and Earth Sciences, Eötvös Loránd University, Budapest, Hungary
[e] Supervisory Authority of Regulatory Affairs, Budapest, Hungary
[f] Department of Meteorology and Geophysics, University of Vienna, Vienna, Austria
[g] Department of Geophysics and Space Science, Institute of Geography and Earth Sciences, Eötvös Loránd University, Budapest, Hungary

ARTICLE INFO

Keywords:
Seismic anisotropy
Shear-wave splitting
Mantle xenoliths
Carpathian-Pannonian region
Tectonic inversion

ABSTRACT

Information on seismic anisotropy in the Earth's mantle can be obtained from (1) shear-wave splitting analyses which allow to distinguish single or multi-layered anisotropy and delay time of the fast and slow polarized wave can indicate its thickness, and (2) studying mantle peridotites where seismic properties can be inferred from lattice preferred orientation of deformed minerals. We provide a detailed shear-wave splitting map of the western part of the Carpathian-Pannonian region (CPR), an extensional basin recently experiencing tectonic inversion, using splitting data. We then compare the results with seismic properties reported from mantle xenoliths to characterize the depth, thickness, and regional differences of the anisotropic layer in the mantle.

Mantle anisotropy is different in the northern and the central/southern part of the western CPR. In the northern part, the lack of azimuthal dependence of the fast split S-wave indicates a single anisotropic layer, which agrees with xenolith data from the Nógrád-Gömör volcanic field. Systematic azimuthal variations in several stations in the central areas point to multiple anisotropic layers, which may be explained by two distinct xenolith subgroups described in the Bakony-Balaton Highland. The shallower layer probably has a 'fossilized' lithospheric structure, representing former asthenospheric flow, whereas the deeper one reflects structures attributed to present-day convergent tectonics, also observed in the regional NW-SE fast S-wave orientations. In the Styrian Basin at the western rim of the CPR, results are ambiguous as shear-wave splitting data hint at the presence of multiple anisotropic layers. Spatial coherency analysis of the splitting parameters places the center of the anisotropic layer at ~140–150 km depth under the Western Carpathians, which implies a total thickness of ~220–240 km. Thicknesses estimated from seismic properties of xenoliths give lower values, pointing to heterogeneously distributed anisotropy or different orientation of the mineral deformation structures.

1. Introduction

Shear waves passing through an anisotropic medium experience splitting into two orthogonally polarized waves. The upper mantle anisotropy is generally attributed to the coherent alignment of olivine and pyroxene due to a prevailing stress regime that promotes the development of lattice preferred orientation (LPO) of these highly anisotropic minerals. Examining P-to-S converted waves at the core-mantle boundary (e.g., PKS, SKS, SKKS; collectively referred to as XKS) allows studying this anisotropy. The delay time between split

* Corresponding author at: MTA FI Lendület Pannon LitH$_2$Oscope Research Group, Institute of Earth Physics and Space Science, Sopron, Hungary.
E-mail address: liptai.nora@epss.hu (N. Liptai).

https://doi.org/10.1016/j.tecto.2022.229643
Received 21 March 2022; Received in revised form 27 October 2022; Accepted 5 November 2022
Available online 13 November 2022

phases and the orientation of fast wave polarization can be a cumulative effect of several anisotropic layers. Nevertheless, these parameters are important proxies to describe the stress and strain regime of the upper mantle and reveal its past and present deformations (e.g., Silver and Chan, 1991; Silver, 1996). Seismic properties such as wave velocities and S-wave anisotropy can be calculated from the LPO of olivine and pyroxenes by using their modal proportions and elastic tensors (Mainprice, 1990). If the sample is representative of the upper mantle, it could yield direct information on the seismic properties of the mantle and can be compared with geophysical observations. Therefore, although seldom combined, the joint study of shear-wave splitting data and seismic properties obtained from deformed mantle rocks holds the potential to contribute to better understanding of mantle anisotropy.

In the western part of the CPR covered by stations included in this study, there are four localities where upper mantle xenoliths were transported to the surface by late Miocene – Pleistocene alkali basalts (Fig. 1): the Styrian Basin, Little Hungarian Plain, Bakony – Balaton Highland, and Nógrád-Gömör (e.g., Szabó et al., 2004). Seismic properties calculated from the LPO were reported by several studies for these locations (Falus, 2004; Hidas et al., 2007; Kovács et al., 2012; Klébesz et al., 2015; Aradi et al., 2017; Liptai et al., 2019), which were used to estimate the thickness of a single anisotropic layer. However, these studies were mainly focusing on local mantle deformation state and history, and while some of them mentioned links to shear-wave splitting results in relation with the studied area, a thorough and detailed comparative study of the greater region is still missing.

Furthermore, a number of papers have addressed how the lithosphere behaves during tectonic inversion in rifted basins such as the Pannonian Basin (Horváth and Cloetingh, 1996; Bada et al., 2007; Dombrádi et al., 2010). Pertinent processes include lithospheric scale folding and accompanying differential vertical variations of surface topography in such inverted basins (Kooi and Cloetingh, 1992). These studies, however, have not investigated the role that the asthenospheric mantle might play in modulating these first order lithospheric processes during tectonic inversion in the Pannonian Basin. Our present study aims to contribute to exploring the potential role of the asthenosphere in the tectonic inversion stage.

The CPR offers a well-documented study area with a variety of tectonic processes in the past few million years, as well as mantle xenoliths hosted in alkali basalts which provide an opportunity for direct analyses. Although the seismic anisotropy of the CPR's upper mantle has been the focus of a number of recent studies (e.g., Qorbani et al., 2016; Song et al., 2019; Petrescu et al., 2020), they did not include interpretations of mantle xenoliths. Therefore, the aim of this paper is to characterize the anisotropy using an increased number of available splitting data and comparing them with seismic patterns described from mantle xenoliths. With the use of this joint geophysical and geological approach, we aim to constrain the deformation and geodynamics of the anisotropic upper mantle in the region.

2. Geophysical background

2.1. Tectonic setting of the Carpathian-Pannonian region (CPR)

The CPR is located in the collision zone of the stable East European Platform (Eurasian Plate) and the Adriatic microplate (Fig. 1). The Pannonian Basin was formed during the Miocene, when the roll-back of a subducting plate promoted the lateral extrusion of the ALCAPA unit (Royden et al., 1982) which rotated counter-clockwise during its eastward movement. It is debated whether the extrusion occurred only on

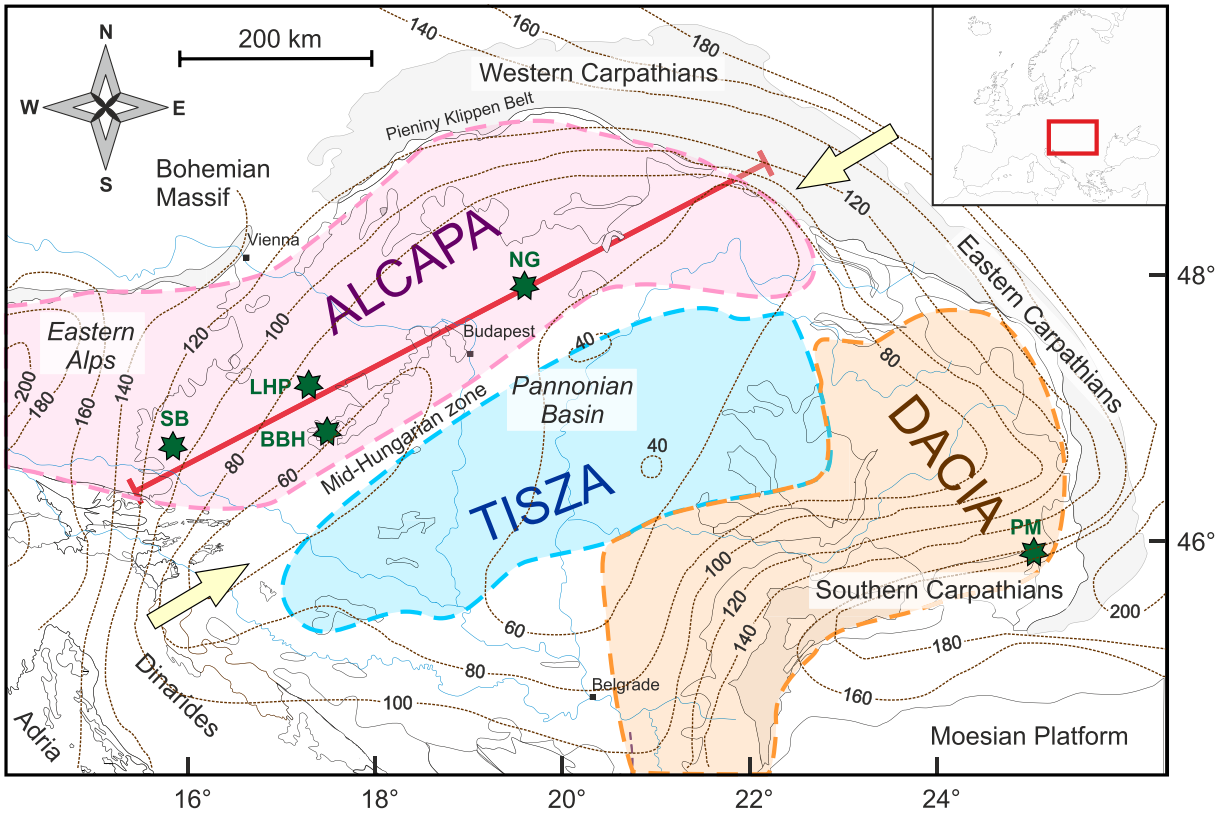

Fig. 1. Structural units of the Carpathian-Pannonian region (modified after Kovács et al., 2007). Lithospheric thicknesses (in km) after Tari et al., 1999 are indicated with dotted lines. Green stars mark the localities of mantle xenoliths hosted in late Miocene-Pleistocene alkali basalt. Red line provides approximate location of schematic sections on Fig. 13. Yellow arrows represent approximate schematic push directions caused by plate convergence. Abbreviations: SB – Styrian Basin, LHP – Little Hungarian Plain, BBH – Bakony-Balaton Highland, NG – Nógrád-Gömör, PM – Persani Mountains. (For interpretation of the references to color in this figure legend, the reader is referred to the web version of this article.)

crustal levels or affected the entire lithosphere. Models proposing gravitational collapse of the Alps or other convergent margins imply that either only the crust takes part in the lateral escape or the entire lithosphere where the crust and lithospheric mantle is coupled (e.g. Ratschbacher et al., 1991; Tari and Horváth, 2010; van Gelder et al., 2017). Some studies (Kovács et al., 2012; van Gelder et al., 2017) argued that the extrusion affected the entire lithosphere in the Alpine orogeny. The southern part of the Pannonian Basin is composed of the Tisza-Dacia unit. During the early Miocene, following the eastward movement and simultaneous clockwise rotation, the Tisza-Dacia became juxtaposed to the ALCAPA microplate along the Mid-Hungarian Zone (MHZ) (Csontos and Vörös, 2004; Schmid et al., 2008).

During the Miocene, large-scale extension caused significant thinning in the entire lithosphere, with a factor of about 1.8–2.7 in case of the crust and of ~4–8 in the lithospheric mantle (Royden et al., 1983). The driving force of the extensionis still under dispute: proposed mechanisms include slab-pull and suction exerted on the upper plate during subduction roll-back (Horváth, 1993; Horváth et al., 2015); eastward directed active asthenospheric flow from the Alpine collision belt (Kovács et al., 2012) and gravitational instability (Houseman and Gemmer, 2007). When the roll-back of the subducted slab ceased upon reaching the stable East European Platform, it resulted in tectonic inversion and gradual shortening of the Pannonian Basin area (Horváth and Cloetingh, 1996; Bada et al., 2007; Dombrádi et al., 2010) starting at ~8 Ma. From the late Miocene (~11 Ma), a series of alkali basaltic volcanism took place in the CPR (e.g., Szabó et al., 1992; Pécskay et al., 1995; Seghedi et al., 2004), bringing xenoliths to the surface from ~8 Ma, which record ambient mantle conditions. Presently, the remnants of this subducted slab may be mapped beneath the Vrancea zone (e.g., Wortel and Spakman, 2000; Koulakov et al., 2009; Martin et al., 2005; Baron and Morelli, 2017; Ferrand and Manea, 2021).

After the cessation of the extension, the north-eastern movement of the Adriatic microplate (with respect to Eurasia) continued, contributing to the tectonic inversion of the basin area (Bada et al., 2007). The effect of the Adriatic push decreases towards the east. While 3.5 mm/yr shortening can be observed in the Adria-Dinarides collision zone and 2.3 mm/yr in the Adria-Alpine collision zone, the Pannonian Basin experiences 1–2 mm/yr shortening (Grenerczy et al., 2005), which defines the main topographical features in the CPR. The absolute plate motion of the Eurasian plate is also in a NE direction (Kreemer et al., 2014).

2.2. Synthesis of existing geophysical data

The Pannonian Basin and the wider Carpathian-Pannonian Region (CPR) have been studied by various shear-wave splitting analyses (Fig. 2) (e.g., Dricker et al., 1999; Ivan et al., 2008; Plomerová et al., 2012; Bokelmann et al., 2013; Paul et al., 2014; Qorbani et al., 2015). The most comprehensive investigations were conducted by Qorbani et al. (2016), Song et al. (2019) and Petrescu et al. (2020). These studies included data from several temporary seismic arrays, such as the Carpathian Basin Project (CBP), and the South Carpathian Project (SCP), resulting in a dense network of splitting measurements. However, there

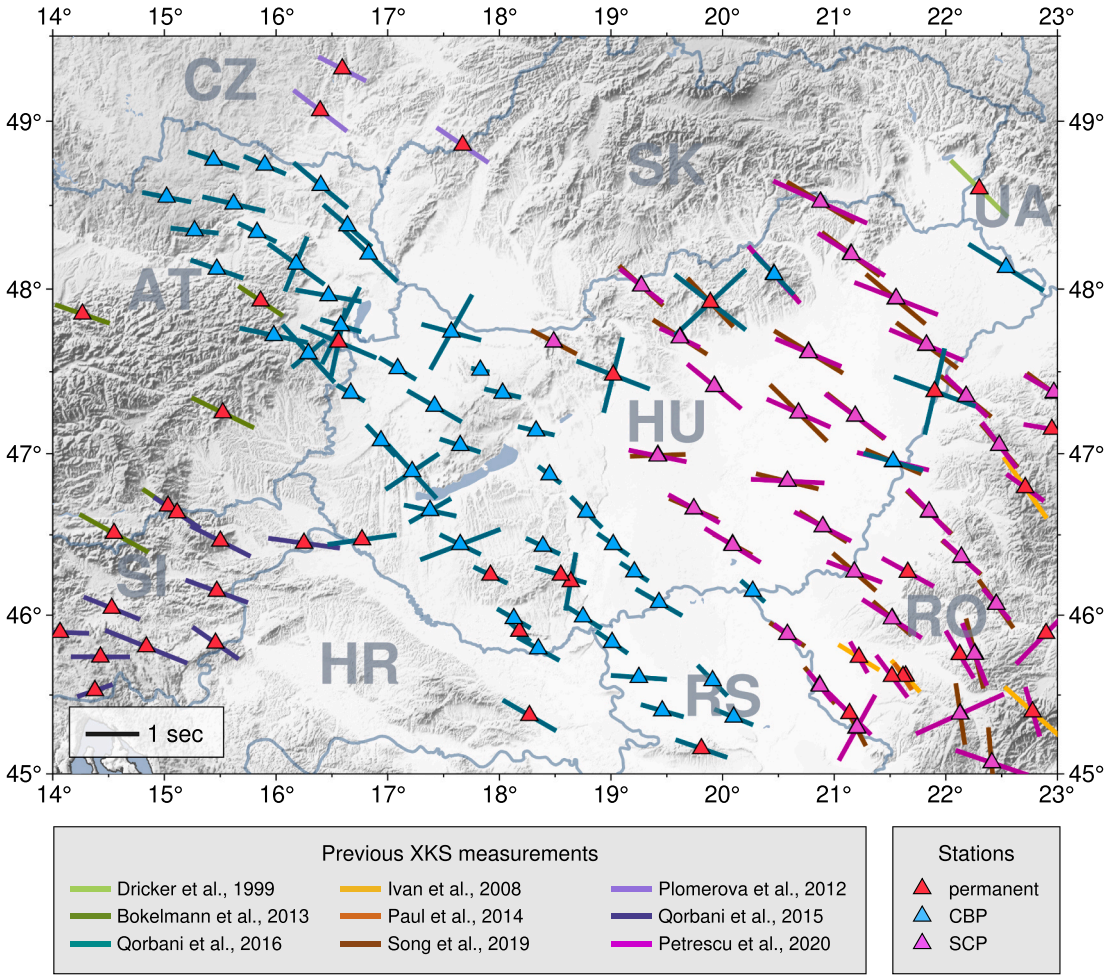

Fig. 2. Previous XKS measurements of the study area and its surroundings. The average fast axis anisotropy bars are colored according to different authors. CBP: Carpathian Basin Project, SCP: South Carpathian Project. Country abbreviations: HU – Hungary, AT – Austria, CZ – Czech Republic, SK – Slovakia, UA – Ukraine, RO – Romania, RS – Republic of Serbia, HR – Croatia, SI – Slovenia.

still remain parts of the transition zone between the Eastern Alps and the Pannonian Basin, where splitting measurements are relatively scarce. Stations of the AlpArray Seismic Network have been operating from around the end of 2015 and the beginning of 2016 (Gráczer et al., 2018; Hetényi et al., 2018). These broadband stations populate the Alpine region and its close surroundings, thus giving an opportunity to fill in the gaps in the datasets. The data collection period of the AlpArray project officially ended in March 2019, but many of the temporary AlpArray stations in the area continued operating (together with the permanent stations), such as the Hungarian and the Austrian AlpArray stations.

Both single layer anisotropy (Song et al., 2019) and possible complex anisotropy (Petrescu et al., 2020) have been proposed beneath the eastern part of the Pannonian Basin. For the western Pannonian Basin, the presence of two-layer anisotropy was suggested by Qorbani et al. (2015, 2016), who have shown a major and a minor anisotropy pattern with different fast axis orientations. However, they could not fit a two-layer model to the observations with the method of Silver and Savage (1994).

The depth of the main anisotropic layer is most often determined by seismic tomography. The 3D model of Zhu and Tromp (2013) shows a complex azimuthally anisotropic pattern beneath Europe. In the CPR at 75 km depth, the fast axis orientations change abruptly from dominantly WNW-ESE in the north to almost NNE-SSW strike in the south. At greater depths, this change is much more smoothly imaged. The strike of the fast axes shows a gradual clockwise change moving from north to south, creating a wide arcuate shape, which follows the strike of a slow shear-wave velocity anomaly beneath central Europe. Although this pattern is unchanged with increasing depth, the magnitude of anisotropy gradually decreases towards greater depths. The maximum anisotropic strength in the Pannonian Basin is mapped at approximately 140–150 km depth (Zhu and Tromp, 2013).

In contrast, spatial coherency analysis of shear-wave splitting measurements identified a depth of the anisotropic layer centered at ~250 km beneath the eastern Pannonian Basin (Song et al., 2019), assuming a single anisotropic layer. Qorbani et al. (2015) detected slab detachment under the Eastern Alps from the SKS measurements, and Qorbani et al. (2016) observed two main fast axis orientations in the western Pannonian Basin. However, the azimuthal coverage of the events for SKS measurements was not sufficient to assess the properties of two anisotropic layers. Similarly, although Petrescu et al. (2020) observed azimuthal dependence of the measurements, they could not specify the parameters of the anisotropic layers in the eastern Pannonian Basin. A certain complexity was also apparent in an application of the alternative splitting intensity method (Hein et al., 2021) for the region, but the overall pattern could still be confirmed.

The uppermost mantle under the Pannonian Basin is characterized by negative P-velocity anomalies (Dando et al., 2011; Ren et al., 2012; Timkó et al., 2019) down to approximately 200 km, accompanied by negative gravity anomalies (e.g., Tašárová et al., 2009) and high surface heat flow (Lenkey, 1999), suggesting a thermal origin and possibly the presence of partial melts (Kovács et al., 2020; Patkó et al., 2021). During the Miocene extension asthenospheric updoming occured thatsignificantly thinned mantle lithosphere (Horváth, 1993). Deep tomographic images (e.g., Dando et al., 2011; Ren et al., 2012) show a north-eastward dipping fast anomaly beneath the Eastern Alps towards the Pannonian Basin. The anomaly continues down into the mantle transition zone, and was interpreted as a remnant of the Adriatic lithosphere subducted beneath the Eurasian plate (Lippitsch et al., 2003), or a remnant of a detached European slab, possibly part of the Alpine-Tethyan lithosphere (Mitterbauer et al., 2011; Qorbani et al., 2015).

2.3. Seismic studies on mantle xenoliths

Although xenoliths from the western part of the CPR were in the focus of numerous studies, only a few papers reported seismic properties calculated from the LPO acquired by electron backscatter diffraction analyses. S-wave velocities and anisotropy calculated from xenolith LPOs are generally used to give an estimate of the thickness of the anisotropic layer in the mantle that produces the delay time in between the fast and slow S-waves on the surface.

In the Styrian Basin and the Nógrád-Gömör volcanic fields, the texture and deformation patterns of the xenoliths did not show evidence for multiple layers in the mantle with different orientation (Aradi et al., 2017; Liptai et al., 2019). Therefore, these authors assumed a single anisotropic layer and concluded that the most realistic scenario is a vertical foliation and horizontal lineation, with a NW-SE orientation. This was deducted from the observed fast S-wave orientations reported by previous shear-wave splitting studies (e.g., Qorbani et al., 2016), interpreted to be a consequence of the transpressional stress field generated by the convergence of the Adria microplate and the Eurasian Plate. The estimated minimum thicknesses were 122 and 125 km for the Styrian Basin and the Nógrád-Gömör, respectively (Aradi et al., 2017, Liptai et al., 2019), which stretch deeper than the lithosphere-asthenosphere boundary (LAB). In both cases, these findings support the suggestion of Qorbani et al. (2016) that a significant contribution to mantle anisotropy is provided by the asthenosphere.

In the Bakony – Balaton Highland, Kovács et al. (2012) distinguished two layers based on petrography, geochemistry and crystal preferred orientation data. They interpreted the shallower layer (~10 km thick) to represent inherited old lithosphere which was thinned during the Miocene extension, and the deeper layer (~ 25 km thick) to represent the uppermost part of the upwelled asthenosphere that 'lithospherized' during the thermal relaxation after the extension. The latter is interpreted to represent present-day stress regimes, whereas the former is suggested to have rather preserved the fossil stress field which is attributed to the west-east directed flow of the asthenosphere. Different explanations have been proposed to constrain the driving force of this asthenospheric flow preceding the tectonic inversion. It could have been an active flow generated as a response to the space problem occurring during the Alpine collision driving the extrusion (Kovács et al., 2012). Alternatively, the asthenospheric flow could have been a passive consequence of either the slab rollback at the eastern margin of the Pannonian Basin, or the opening of the Dinaric slab gap (Handy et al., 2015; Horváth et al., 2015). Nevertheless, the fossilized mantle structure may explain the *E*-W directed fast polarization orientations observed by SKS splitting studies in the region (Qorbani et al., 2016; Kovács et al., 2012 and references therein). Calculated thicknesses for the anisotropic layer are in the range of 85–115 km, taking into account only the deeper layer as the shallower layer was suggested to play a negligible role (Kovács et al., 2012). These depths suggest an asthenospheric contribution to the anisotropic layer, similarly to the Styrian Basin and the Nógrád-Gömör.

3. Collection and analysis of newly acquired geophysical data

Previous shear-wave splitting studies have analyzed the recordings of the CBP, SCP and most of the permanent stations in the Pannonian Basin. As part of the Hungarian National Seismological Network (HNSN, doi:10.14470/UH028726) several temporary and permanent stations have been deployed in the last few years. This has provided an opportunity to significantly increase the number of splitting measurements, while newly available misorientation data of the stations allowed us to account for them when measuring the shear-wave splitting parameters.

The Hungarian seismological stations have been deployed using a magnetic compass. In 2018, we could use a gyrocompass in order to measure orientation for existing stations all over the country. Their misorientation varied between −14.6° and 18.9° (Gráczer et al., 2018). We have also retrieved orientation measurements from the station metadata in case of the Austrian and Slovakian AlpArray stations. Unlike previous studies, we took into consideration these misorientation values. We used data from 15 permanent and 28 temporary stations located in Hungary, Slovakia (doi:10.14470/FX099882), Austria and

Croatia, in the area of the transition zone between the Eastern Alps and the Pannonian Basin (Fig. 3). Data of the stations located in the eastern Pannonian Basin were processed by Song et al. (2019) and by Petrescu et al. (2020). However, as both studies left out two permanent broadband stations: AMBH and BSZH, we also included these stations in our study.

In order to maximize the number of splitting measurements, we have analyzed teleseismic events in an epicentral distance range from 84° to 180° with magnitudes >5.75 (M_w). Waveforms were bandpass filtered prior to further processing. Corner frequencies were selected based on visual inspection of the waveforms in order to obtain the most clear split. An upper corner frequency of 0.4 Hz was applied almost exclusively, while 0.04 Hz was chosen for the lower corner frequency in ~60% of the measurements and 0.1 Hz was used in ~40% of the cases. Careful selection of the measurement window ensured optimal splitting and only measurements with clear splitting were accepted. Data were processed from the very beginning of each station operation until 30.06.2020. both for temporary and permanent stations. During the data collection period three stations (A268A, A269A, A270A) were renamed (HU08A, HU09A, HU10A, respectively) in the frame of the international PACASE (Pannonian-Carpathian-Alpine Seismic Experiment) project. The PACASE project is carried out as a new "AlpArray Complementary Experiment", with the contribution of 7 countries and started in 2019. Nevertheless, Fig. 3 shows the original names of the stations.

The *SplitLab* software of Wüstefeld et al. (2008) was used for the shear-wave splitting measurements. Fast polarization axis orientation (φ) and delay time (δt) between fast and slow phases were calculated by minimizing the energy on the corrected transverse component (Silver and Chan, 1991). Quality was ensured based on the following criteria: (1) XKS arrival clearly visible on the original radial and transverse component (2) almost perfect energy removal on the corrected T component (3) the similarity of the corrected fast and slow waves (4) ellipticity of the particle motion before and after correction (5) well defined minimum on the contour map and (6) stability of the measurement. A measurement was accepted only if it satisfied most of the above criteria. Therefore, even poor measurements can be valid, possibly with greater uncertainty or less perfect energy removal from the transverse component. Similarly to the measurements, classification was carried out manually, which is inevitably subjective. As the results show very coherent orientations regardless of their assigned quality, we do not differentiate between the good, fair, and poor measurements.

The measurements with no splitting of the XKS phase are called Null measurements. Theoretically, this can either mean that the wave has not traversed an anisotropic medium, or in most cases, the incoming wave path (the backazimuth of the event) is parallel to the fast or slow axis orientation. However, Liu and Gao (2013) have argued that many measured Nulls are a result of energy of the transverse component smoothing into the background noise, and for most forms of complex anisotropy Null measurements are rarely observed. Furthermore, their synthetic tests have shown that pure Null measurements are non-existent in case of complex anisotropy. Considering the above, as signs of complex anisotropy were present at some of the processed stations, we did not examine further the observed Null measurements.

Assuming a single anisotropic layer in the mantle, its thickness can be estimated from the velocities and the delay time between the fast and slow S-wave (Pera et al., 2003). The thickness of the anisotropic layer in the mantle is largely influenced by the spatial orientation of the foliation (layering) and the lineation (parallel aligned structural elements representing the direction of maximum elongation) of the deformed mantle peridotite (Baptiste and Tommasi, 2014). In the majority of cases, this cannot be determined from the xenoliths. For different scenarios, five endmember cases can be distinguished, as proposed by Baptiste and Tommasi (2014): horizontal foliation and lineation (case 1), vertical foliation and horizontal lineation (case 2), vertical foliation and lineation (case 3), 45° dipping foliation and lineation (case 4), and 45° dipping foliation and horizontal lineation (case 5).

Using the delay times of the fast and slow S-wave detected on the surface by the nearest station, a thickness (T) in km can be calculated

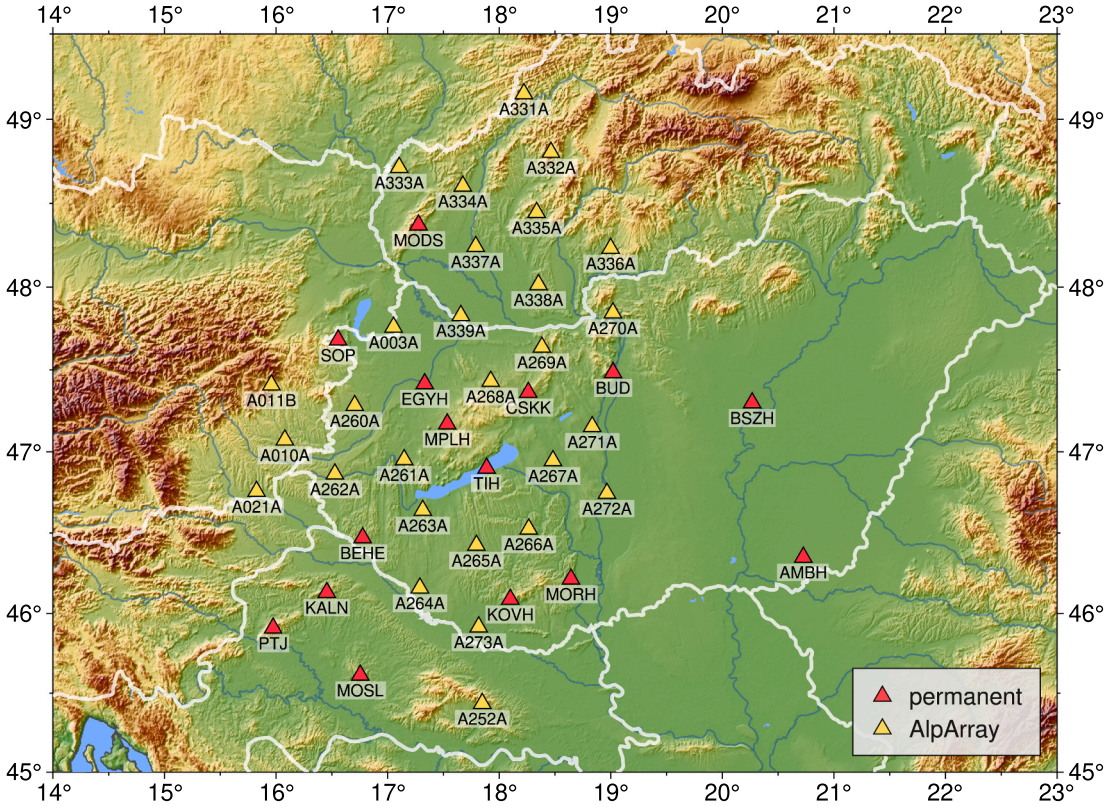

Fig. 3. Seismic stations used for shear-wave splitting measurements.

using the following equation (Pera et al., 2003):

$$T = 100dt^{*}\frac{Vs_a}{AVs}$$

where dt is the delay time (s), Vs_a is the average of the fast and slow velocities (km/s), and AVs is the anisotropy for a specific propagation direction expressed in percentages (%). The 3D distribution of AVs and the two S-wave velocities can be obtained using the LPO of olivine and pyroxenes (Mainprice, 1990). The S-velocities and AVs are commonly plotted on pole figures with respect to the foliation and lineation, and thus their values for vertical propagation depend on where the vertical direction is positioned compared to the foliation and the lineation. For a more detailed illustration on how to obtain these seismic properties in the different orientation scenarios, see Fig. 6 of Klébesz et al., 2015.

4. Results

At 43 stations, 1122 pairs of splitting parameters were measured altogether, among which 109 are PKS, 746 are SKS, 251 are SKKS (Fig. 4), 15 are SKiKS and one is SKJKS measurement. Observed fast polarizations are oriented in an approximately WNW-ESE orientation (Fig. 5). They rotate gradually from NW-SE in the Western Carpathians to almost *E*-W in central western Hungary. The majority of the fast polarization orientations ranges between 80° and 150° (Fig. 6a). The delay times show a pronounced variation (Fig. 6b), with mean values for each station varying between 0.69 s and 1.48 s, suggesting significant lateral thickness variation of the anisotropic layer.

4.1. Station-averaged splitting parameters

Our results are consistent with previous studies, demonstrating that the prevailing anisotropic pattern is WNW-ESE in the Pannonian Basin. This pattern is not correlated with the absolute plate motion direction (marked by purple arrows in Fig. 7a; Kreemer et al., 2014), but is roughly parallel to the Teisseyre-Tornquist Zone (East European Platform margin). In Fig. 7, the results of previous measurements are combined and plotted together with the splitting parameters of this study. For stations where multiple authors have published shear-wave splitting measurement results, the circular mean of the orientations is given, while δt is averaged. For stations where we reprocessed all available data (e.g., BUD), we favored our new results as they are derived from a longer observation period. Some of the measurements were controversial, as Qorbani et al. (2016) identified two fast polarization orientations at several stations. Although usually, we have accepted the main pattern, in case the minor pattern was more similar to the orientations that we have determined, we used the latter for further interpretation. As only one individual splitting measurement was published by Qorbani et al. (2016) at station CBP4I, which was contradictory to our results in its vicinity, we have omitted this station from further evaluation.

Based on the combined dataset of XKS splitting parameters in the Pannonian Basin, two distinct regions could be localized (encircled in Fig. 7b), where orientations differ significantly. This region, marked by blueish colors in Fig. 7b shows an ENE-WSW–E-W fast orientation. On the other hand, at the Western Carpathians (reddish colors) more of an ESE-WNW orientation was measured. Nevertheless, these regions are not reflected in the color-coded map of the delay times (Fig. 7b, inset). In general, the observed delay times are larger in the northeastern part of the Pannonian Basin than in the southwest.

Shear-wave splitting measurements are carried out using individual teleseismic events. As such, a single event might provide sound splitting parameters for many seismic stations. During the processing, we found that some of the studied events produce remarkably good results, similar to the station average. The best events and their splitting parameters are shown in Fig. 8. A question remains whether the earthquake locations and the fast axis orientations or the source parameters are responsible for this phenomenon. The listed earthquakes occurred at 196 km, 510 km and 169 km depth (in chronological order) and their magnitude (M_W) was 7.7, 6.3, 6.8, respectively. Their most striking feature in common is their backazimuth, which forms an angle of approximately 60° with the average fast axis orientation in the western Pannonian Basin.

4.2. Depth of anisotropy

The results of shear-wave splitting measurements are usually interpreted under the assumption of a single homogeneous anisotropic layer of hexagonally symmetric material with a horizontal symmetry axis (Silver, 1996), as flow-induced alignment of olivine within the upper mantle or fossil lithospheric fabric.

If multiple anisotropic layers are present, fast polarization axis orientations show systematic azimuthal variations. To represent the spatial distribution of regions with simple or complex anisotropy, we have created a complex anisotropy index map (Fig. 9) after Yang et al. (2014) based on the azimuthal dependence of the observed fast axis orientations (Fig. . S1 in the Supplementary information). Stations have been classified depending on whether systematic azimuthal variations could or could not be observed. At some stations, the azimuthal coverage is still not sufficient to decide if simple or complex anisotropy is present beneath the station. However, in the Western Carpathians, a relatively consistent pattern can be observed, as none of the stations show obvious

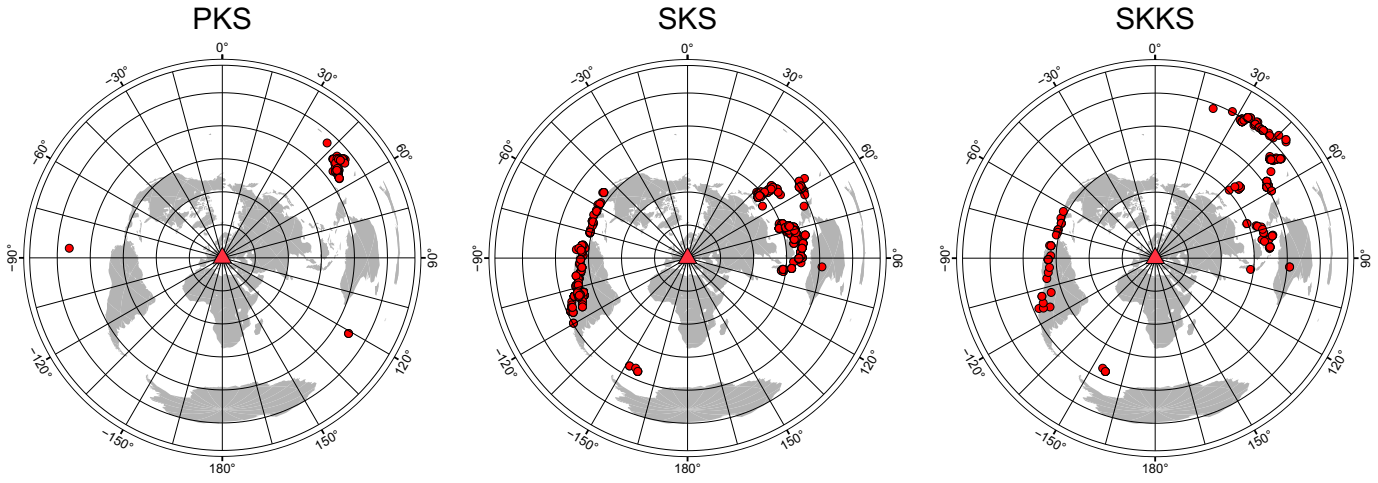

Fig. 4. Epicenter distribution of events used for PKS, SKS and SKKS measurements.

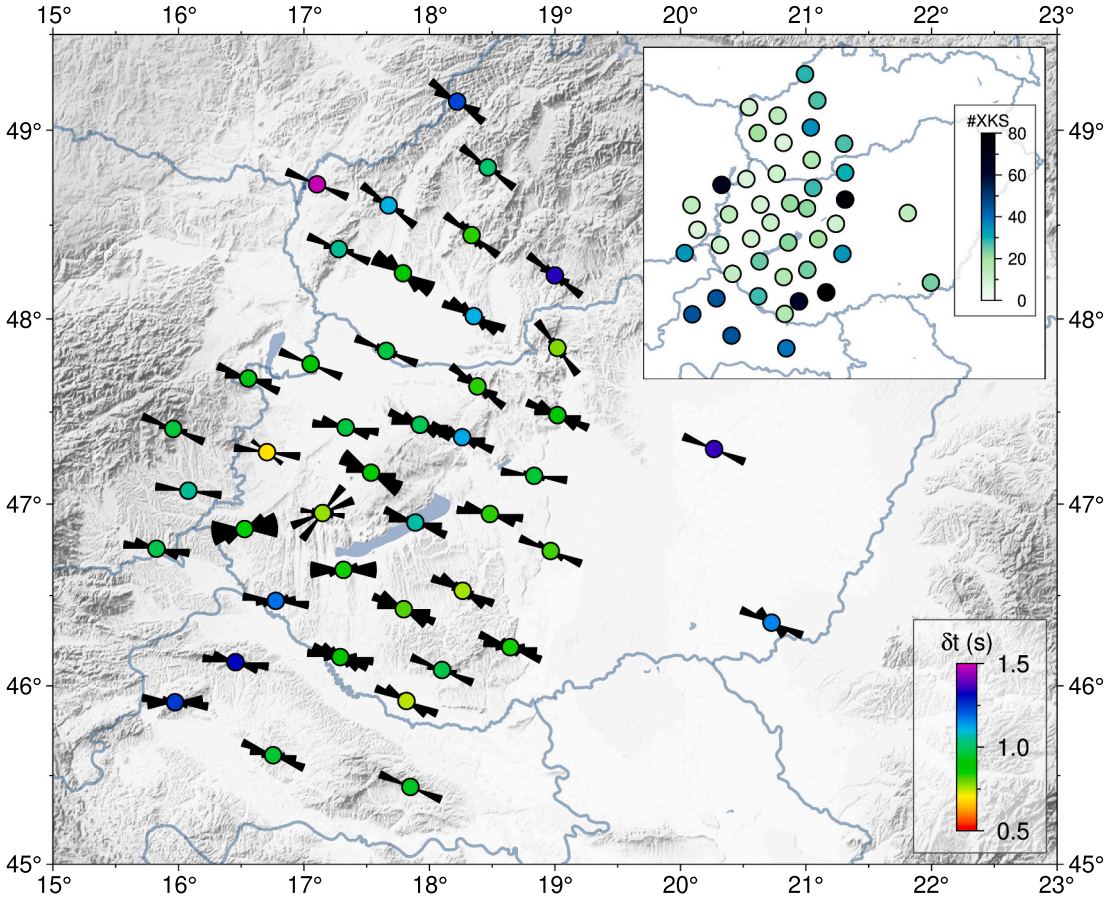

Fig. 5. XKS fast axis orientation measurements are shown as rose histograms with circles colored according to average delay time. Inset: number of XKS measurements for each station. (For interpretation of the references to color in this figure legend, the reader is referred to the web version of this article.)

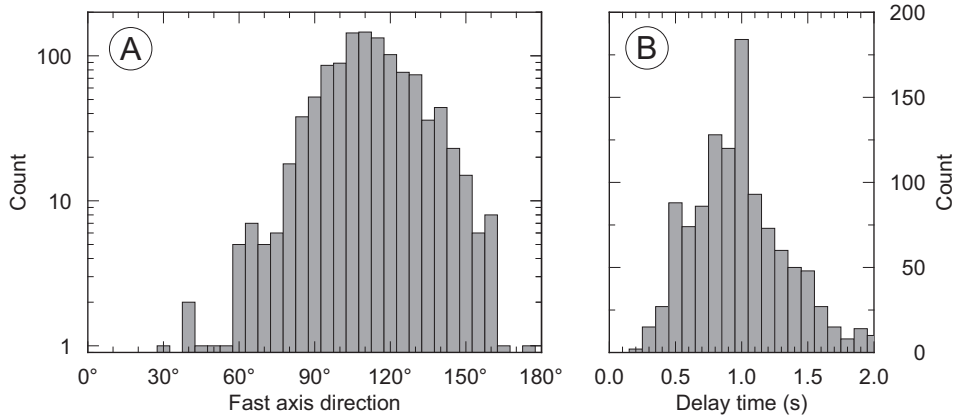

Fig. 6. Histograms of observed fast polarization orientations (A) and delay times (B). Fast axis orientations cluster around 110°. The most common delay time is 1.0 s.

azimuthal dependence. Fig. 10 shows the backazimuth versus fast axis orientations for these AlpArray stations in the Western Carpathians. Although the average fast axis orientation might slightly vary for these stations, none of them shows significant azimuthal dependence, which suggests simple anisotropy in the area.

In case of simple anisotropy, by measuring the spatial coherency of the splitting parameters applied to different depths, it might be possible to estimate the depth of the anisotropic layer (Liu and Gao, 2011). We have applied this method to the 159 measurements at the 8 stations in the Western Carpathians (Fig. 10). The analysis shows that the center of the anisotropic layer lies at approximately 140–150 km depth (Fig. 11), which agrees well with findings of Zhu and Tromp (2013), who found maximum anisotropy beneath the wider Pannonian Basin area at this depth range.

4.3. *Thickness of the anisotropic layer based on mantle xenolith data*

We have re-calculated the thickness of the anisotropic layer for the xenoliths with available seismic data from the Styrian Basin, Little Hungarian Plain, Bakony-Balaton Highland and Nógrád-Gömör volcanic

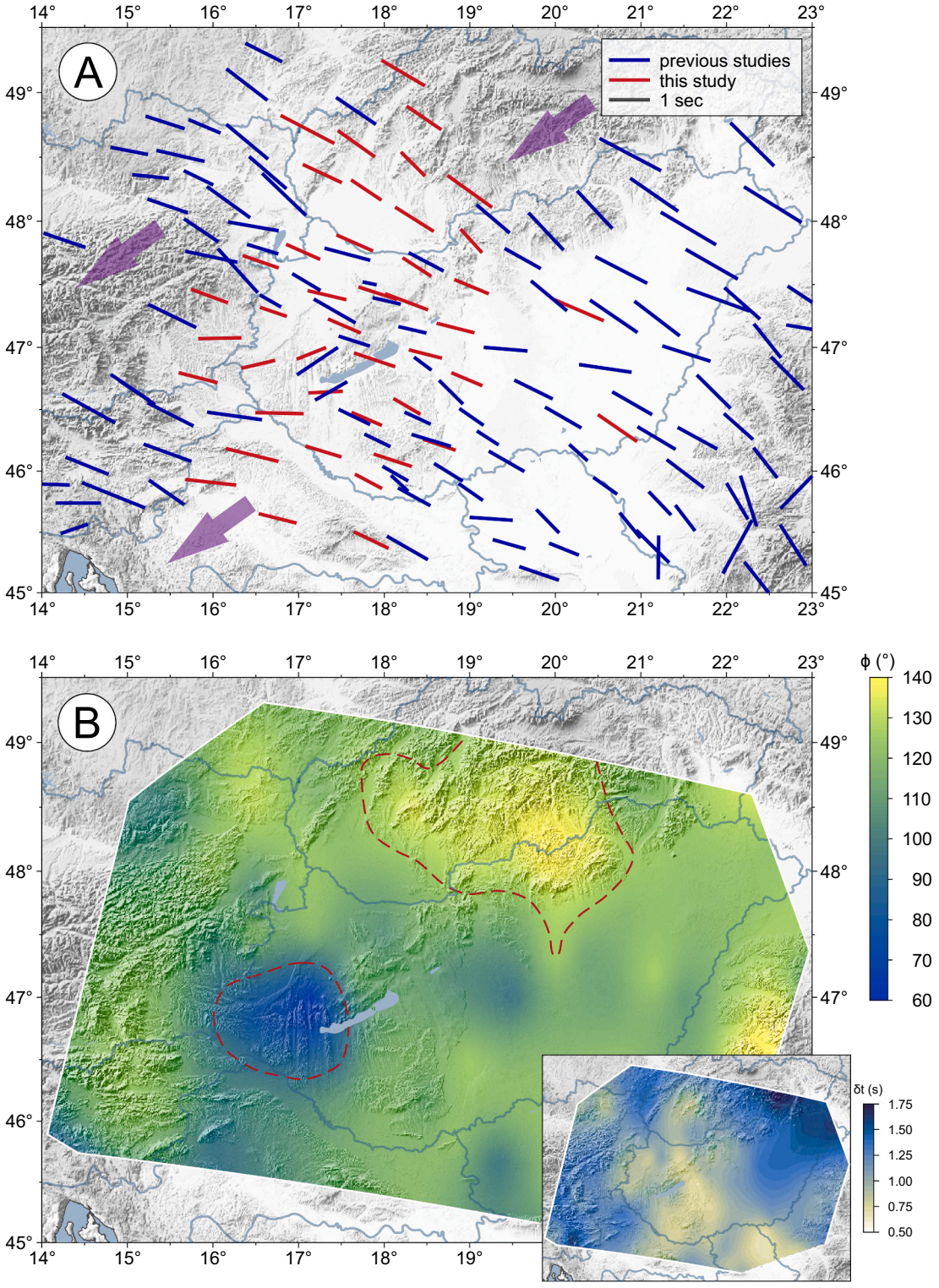

Fig. 7. A - Published and new shear-wave splitting measurements for each station. The orientation of the anisotropy bars shows the average fast axis orientation, while their length corresponds to delay times. The thick arrows show the absolute plate motion directions according to Kreemer et al. (2014). B - Color coded map of fast polarization orientations in the study area. Dashed lines correspond to 95° and 125° fast orientations. Inset: color coded map of delay times.

fields (Table S1 in the Supplementary information). We used the newly reported delay times at stations A010A (1.05 s), A260A (0.69 s), TIH (1.06 s), and A336A (1.34 s) (Fig. 3.; 5), respectively for the xenolith localities. Note that these delay times are in agreement with those previously used for the Bakony-Balaton Highland (~1 s; Kovács et al., 2012) and the Nógrád-Gömör (1.3 s; Liptai et al., 2019), whereas delay times are slightly shorter for the Styrian Basin (1.27; Qorbani et al., 2015; Aradi et al., 2017).

An important question arises whether it is worthwhile estimating the thickness of a single anisotropic layer in localities where multiple layers are assumed, such as in the Bakony-Balaton Highland and Little Hungarian Plain (Kovács et al., 2012). However, if both the foliation and the

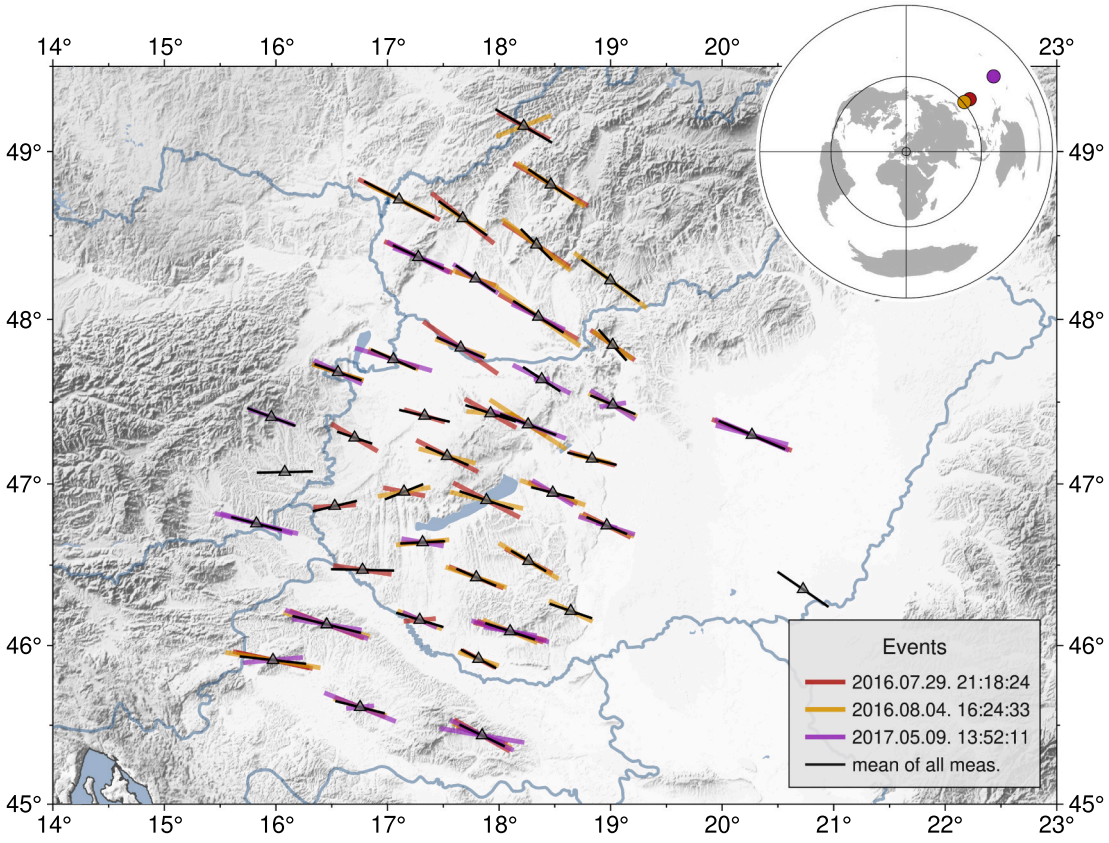

Fig. 8. Splitting parameters measured using the listed events (see inset for locations) and means of all measurements for each station.

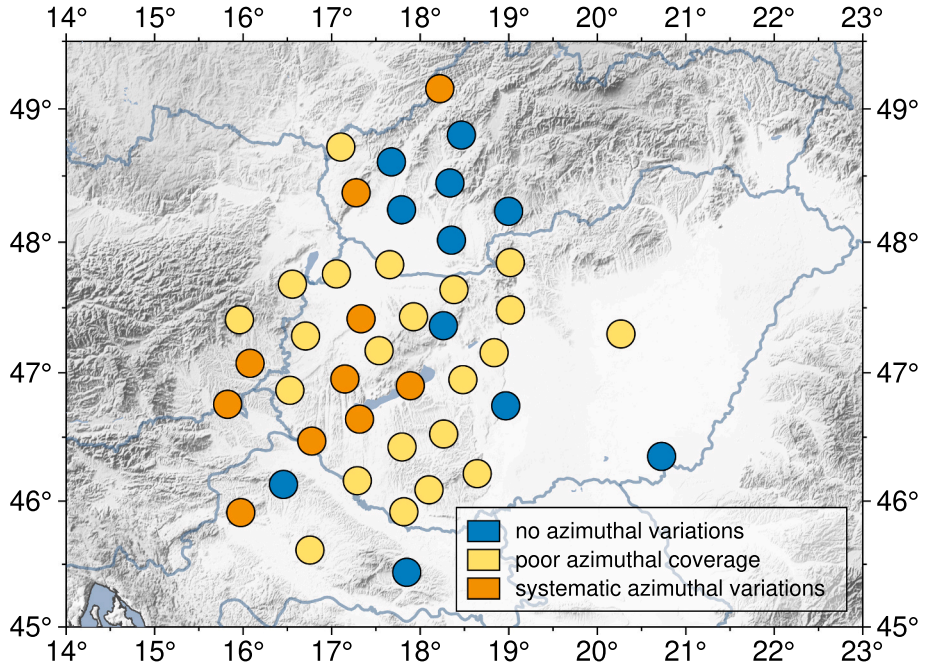

Fig. 9. Anisotropy index map based on visual inspection of azimuthal dependence of fast axis orientations.

lineation is oriented horizontally (case 1), as suggested for the shallower layer, there is no or only negligible anisotropy for the vertically propagating S-waves. Consequently, this layer will not (or only minimally) contribute to the overall delay time, whereas calculated thicknesses of an anisotropic layer would be unrealistically high. Therefore, as Kovács et al. (2012) suggested, this layer was ignored and the thickness was calculated using data of xenoliths originating from the deeper layer only, where a significant S-wave anisotropy is present due to the vertical foliation and horizontal lineation (case 2). These only include xenoliths from the Bakony-Balaton Highland, as those from the Little Hungarian

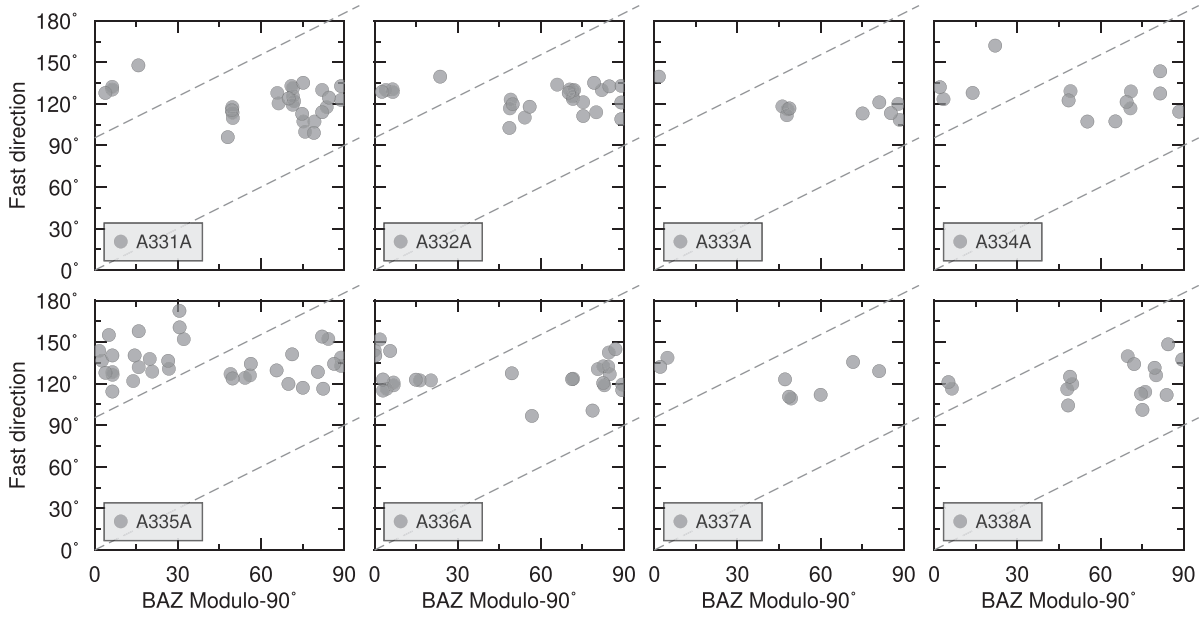

Fig. 10. Azimuthal dependence of fast polarization orientations for stations in the Western Carpathians. Although the average fast orientations might slightly differ for these stations, none of them show obvious azimuthal dependence.

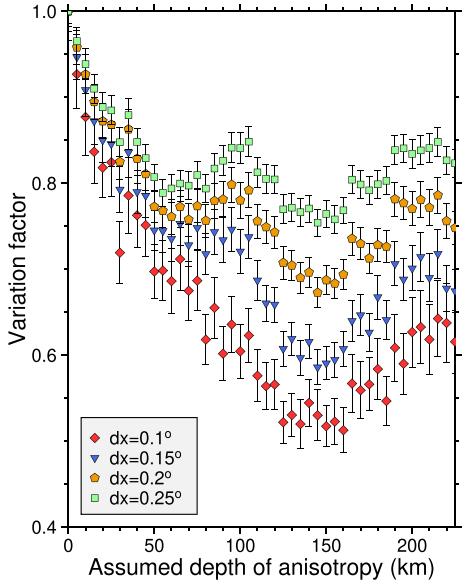

Fig. 11. Spatial coherency analysis of splitting parameters based on 8 AlpArray stations located in the Western Carpathians. The location of the minimum value of the variation factor corresponds to the central depth of the anisotropic layer at about 140–150 km assuming single layer anisotropy.

Plain are assumed to represent the shallower layer. To increase the number of samples, we have included four additional xenoliths from Füzes-tó quarry within the Bakony-Balaton Highland, all having equilibrium temperatures over 1050 °C which points to their deeper origin (Liptai et al., 2021).

The re-calculated thicknesses for case 2 scenarios resulted in 65–290 (with an average of 109) km for the Styrian Basin, 92–222 (with an average of 137) km for the Nógrád-Gömör, and 67–168 (with an average of 97) km for the Bakony-Balaton Highland. Note that the contribution of the crust is ignored in this calculation, as it is well known that the crustal contribution in shear-wave splitting measurements is significantly smaller than the effect of the mantle. It is generally accepted that the crustal contribution to the total delay time is typically about 0.1 s per 10 km (Silver, 1996; Barruol and Mainprice, 1993). Therefore it follows that more significant contribution can be expected in areas with thick continental crust (Latifi et al., 2018). However, since the Carpathian-Pannonian region is characterized by a thin crust in general (<30 km; Horváth, 1993; Kalmár et al., 2021), the crustal contribution to surface delay times was usually ignored in SWS splitting analyses in the area (e.g., Qorbani et al., 2016; Petrescu et al., 2020). In a previous study of the Nógrád-Gömör xenoliths (Liptai et al., 2019), the authors attributed a ~ 0.25 s of the delay time to the crust; however, this is well below the delay time of the A336A station closest to the xenolith locality. Furthermore, without the examination of potentially complex crustal structures, it appears appropriate to assume that our delay time values mainly refer to a mantle source.

5. Discussion

The lithospheric anisotropy might be frozen in from previous tectonic processes (Silver and Chan, 1991; Tommasi and Vauchez, 2015; Plomerová et al., 1996; Plomerová et al., 2007). Although the basement of the Pannonian Basin consists of two terrains with different origin and history, and the ALCAPA and Tisza micro-terrains rotated in opposite directions during the Miocene extension, the determined fast axis orientations do not change significantly through the transition of different micro-terrains. This suggests that the impact of relative motion is already overprinted by more recent geodynamic processes. Another possibility is that the observed pattern originates from greater depths and is not related to the two major lithospheric units building up the basement of the Carpathian Pannonian region.

Despite the notion that anisotropic patterns may take some time to develop in the lithosphere, Zhu and Tromp (2013) have reported that the anisotropic fabric in the upper mantle beneath Europe is generally consistent with present-day surface-strain rates derived from geodetic measurements. Coherent fast axis orientation and absolute plate motion direction can be interpreted as a result of coupling between the lithosphere and asthenosphere, causing simple shear between them. However, this appears not to be the case for the study area, as fast axis orientations tend to be closer to perpendicular to the plate motion direction rather than being parallel to it.

5.1. Comparison of seismic data from shear-wave splitting and mantle xenoliths

Although for some stations, the azimuthal coverage was not sufficient to determine whether there is a single or multi-layered anisotropy, it appears there is a difference between the northern and central-southern parts of the covered area, i.e., the western CPR. In the northern part, especially under the Western Carpathians, a single anisotropic layer can be assumed from the lack of systematic azimuthal variations in most of the stations (Figs. 9, 10). This is in agreement with the fact that the xenoliths of the Nógrád-Gömör volcanic field do not show evidence of depth-related layering in terms of their petrography or LPO. In contrast, the variability in their texture and composition was attributed to the different ages and spatial distribution (Liptai et al., 2017, 2019). However, in the central and southern regions of the western CPR, including basin areas and the transition zone towards the Eastern Alps, more stations indicate multi-layered anisotropy, especially in the vicinity of Lake Balaton (Fig. 9). This is in agreement with the Bakony-Balaton Highland xenoliths described in the study of Kovács et al. (2012), which clearly show two different layers in terms of texture and olivine LPO pattern, a shallower layer with 'axial-010' and a deeper one with 'A-type orthorhombic' patterns. Their suggestion that the shallower layer represents the uppermost part of the asthenospheric dome that was lithospherized following the cessation of the extension, can explain why multi-layered anisotropy is only detected in the central, most thinned part of the Pannonian Basin which was subject to more intensive extension in contrast to marginal areas such as the Western Carpathians. It should be noted that in the central-southern Pannonian Basin, there are many stations with poor azimuthal coverage, and even a few which suggest single-layered anisotropy. It is possible that this is because the extension-driven thinning of the lithosphere was not uniform throughout the whole basin, and thus the spatial distribution of single or multi-layered anisotropy is more heterogeneous than previously thought.

The Styrian Basin is not as straightforward as the other two xenolith localities. Stations A010A and A021A, located closest to the xenolith-hosting alkali basalt outcrops, both show azimuthal variations and thus suggest multiple anisotropy. Although no clear layering was observed based on the petrography and LPO of the xenoliths (Aradi et al., 2017), some correlation can be observed between their LPO-pattern and equilibrium temperature: xenoliths with lower equilibrium temperature (i.e., shallower depth of origin) dominantly show 'axial-010' type LPO pattern, whereas higher temperature (deeper) xenoliths have more 'orthorhombic' type pattern among them (see Fig. 6b of Aradi et al., 2017). While the distribution is rather transitional with several outliers as well, this correlation is the same as in the case of the Bakony-Balaton Highland (and Little Hungarian Plain) xenoliths (Kovács et al., 2012). However, the two layers may not be separated as clearly under the Styrian Basin as under the Bakony-Balaton Highland, and the transition between the two could spread more evenly or across a greater vertical distance.

Another explanation may be connected to the complex tectonic nature of the Styrian Basin, located above a former subduction zone, and the edge of the extensional basin, which means that the lithosphere-asthenosphere boundary (LAB) may be tilted considerably instead of being (sub-)horizontal. Based on shear-wave splitting analyses of the Eastern Alpine region and a comparison with tomographic studies, Qorbani et al. (2015) suggested the presence of a detached slab of the European plate at depths in the excess of 300 km, which represents the deeper one of two anisotropic layers. According to their suggestion, the slab may be connected with the lithosphere under the Eastern Alps, and possibly with the slab graveyard towards the east. This could explain the observed multiple anisotropy in the area of the Styrian Basin (Fig. 9), and may also link to the fast orientation anomaly detected in the western part of Hungary, between the Eastern Alps and the Transdanubian Range (Fig. 7b). Although Qorbani et al. (2015) found that fast orientations in the detached slab are SW-NE under the Eastern Alps, the anomaly seen on Fig. 7b is located more to the east without overlapping with their study area. The *E*-W fast orientations may thus be explained by the slight rotation of the eastward sinking slab and/or its pulling effect on the overlying mantle. Furthermore, since the location of this detached slab is estimated to be at or below ~300 km, it appears to be reasonable to calculate the thickness of the above laying anisotropic layer from the Styrian Basin xenoliths assuming single anisotropy.

5.2. Dimensions of the anisotropic layer(s) in the mantle

Beneath the Western Carpathians, where a single anisotropic layer is assumed, results of the spatial coherency analysis suggested that the center of the anisotropic layer is at ~140–150 km depth (Fig. 11). If we adopt a thickness of ~30 km for the crust (e.g., Horváth, 1993; Kalmár et al., 2021), this corresponds to 110–120 km between the Moho and the suggested center at ~140–150 km. If the same amount is assumed below this center, the total thickness of the anisotropic layer adds up to 220–240 km, under the crust, with the bottom located at ~250–270 km below the surface. This may mark the bottom of the low velocity zone (the ductile, upper part of the asthenosphere which is considered to contain small amounts of partial melt; Green, 2015), expected to be at greater depths in hot, active areas (250–400 km; Thybo, 2006) such as the CPR, in contrast to cold, stable areas. Note that this is a maximum thickness for the anisotropic layer, if we assume that the anisotropy is present in the mantle up to the Moho. The latter is supported by the sampling depth of the xenoliths close to the Moho between 35 and 50 km (Liptai et al., 2017).

This 220–240 km of total anisotropic thickness inferred from the spatial coherency analysis is significantly greater than the average (137 km) and closer to the maximum (222 km) thickness calculated from seismic properties of Nógrád-Gömör xenoliths. This, along with the wide variability of textures and LPO patterns of the xenoliths (Liptai et al., 2019) supports earlier findings that the upper mantle sampled by the xenoliths is strongly heterogeneous. One possibility is that the xenoliths with lower S-wave anisotropy, which result in a thicker anisotropic layer, are a better representation of the depth range underlying the source region of the xenoliths.

The other factor that should be taken into account, is the orientation of mantle structures (foliation and lineation). The above-mentioned thickness values were obtained assuming vertical foliation and horizontal lineation (case 2), which can be expected in a compressional regime. Case 2 produces the strongest S-wave anisotropies and thus the calculated thickness is the smallest compared to the other cases (e.g., Aradi et al., 2017; Liptai et al., 2019). Although this is the most likely scenario, in a natural environment the orientations of the foliation and lineation may not perfectly and/or homogeneously represent an ideal case 2. Their orientation may be somewhat oblique and it may also vary spatially. Out of the rest of the endmembers, case 5 (45° dipping foliation and horizontal lineation) is the second most plausible, as it would also result in NW-SE directed fast polarizations and the second lowest calculated thicknesses. Assuming case 5, calculated thicknesses from Nógrád-Gömör xenoliths range from 107 to 320 (with an average of 193) km (Table S1), which are still realistic. Furthermore, thicknesses calculated for the two endmembers correlate well in individual xenoliths (Fig. 12). In summary, we suggest that the orientations of the foliation and lineation in the anisotropic mantle layer may vary between case 2 and 5, i.e., horizontal lineation and slightly dipping but likely close to vertical foliation.

It is noteworthy that the olivine LPO pattern may also influence delay times detected on the surface, and thus the estimated thickness of the anisotropic layer. Recently, Löberich et al. (2021) proposed that under the southern Cascadia back-arc system, olivine fabrics have more likely E- than A-type patterns based on azimuthal variations of splitting parameters. E-type fabric is similar to A-type in the sense that the distribution of all three olivine crystal axes have single maxima, but their

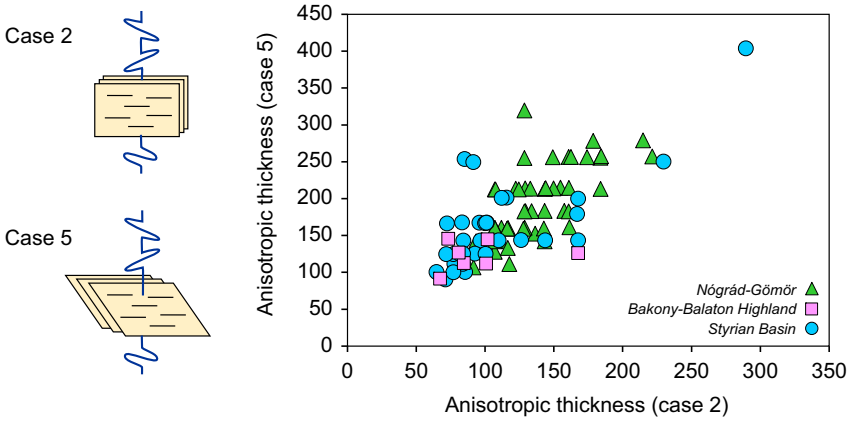

Fig. 12. Comparison of thicknesses (km) of the anisotropic layer calculated from xenoliths of the different localities, assuming vertical foliation + horizontal lineation (case 2) and 45° dipping foliation + horizontal lineation (case 5).

orientation is different with respect to the foliation and lineation. Furthermore, the E-type is suggested to develop under more hydrous conditions compared to the A-type (Jung et al., 2006 and references therein). However, none of the xenoliths of the CPR have been described as E-type as fabrics with single crystal maxima were determined as A-type due to the orientation of the axes with respect to the foliation and lineation (Kovács et al., 2012; Aradi et al., 2017; Liptai et al., 2019). Furthermore, extremely low water contents in xenoliths, especially from the Nógrád-Gömör and Bakony-Balaton Highland (Patkó et al., 2019) also support the development of A-type fabrics. Thus this scenario involving E-type pattern seems rather unlikely for the study area.

In the Bakony-Balaton Highland, the calculated thicknesses are significantly lower (67–168 with an average of 97 km for case 2, and 92–146 with an average of 123 km for case 5) than in the Nógrád-Gömör, even though this excludes the uppermost ~10 km of the mantle whose contribution to shear-wave splitting can be neglected. In the Styrian Basin, thickness ranges are similar to that of the Nógrád-Gömör (65–290 km for case 2, 90–404 km for case 5; by excluding one outlier, the greatest thicknesses are 230 and 254 km for cases 2 and 5, respectively). This may indicate that the anisotropic layer is thinner in the central than in the northern and western part of the CPR, or that the xenoliths used for the calculation do not accurately represent the whole depth range of the anisotropic layer. It is also possible that a higher level of extension produced more significant anisotropy in the central part than in the marginal areas.

5.3. The role of 'asthenospheric jam' on the orogenic rim

The measured shear-wave splitting data imply that the asthenosphere beneath the Carpathian-Pannonian region is usually vertically or sub-vertically foliated and that the lineation is mainly horizontal. This fabric in the asthenosphere might have been developed at least in part as a response to tectonic inversion (Qorbani et al., 2016; Kovács et al., 2020). During the tectonic inversion, the asthenospheric dome got trapped between the thicker Adriatic and European lithospheres on the SW and NE, respectively (Kovács et al., 2020). The convergence between these plates and the counter-clockwise rotation of Adria is responsible for the perpendicularly developing NW-SE directed vertical, sub-vertical foliation. According to the measurements of Bus et al. (2009), the degree of shortening is ~1,3 mm/a between the Alpine foothills and the Danube bend. This translates to a shortening of ~6,5 km in this area during the inversion. This estimate bears significant uncertainties, but highlights that even a shortening of this magnitude must have resulted in the displacement of a significant volume of asthenospheric material between the converging Adriatic and European lithospheres. This asthenospheric material under compression either "leaves" the asthenospheric dome perpendicular to the compression or may contribute to further uplifts in the basin, as seen for example for the Transdanubian central range (Ruszkiczay-Rüdiger et al., 2020). This also means that the asthenospheric dome under compression generates a stress field in which asthenospheric material is forced to escape along the surrounding orogenic rim of the Carpathian-Pannonian region, perpendicular to the major NE-SW compression (Fig. 13). This asthenospheric jam may contribute to what is observed in the SE Carpathians, where the change in Moho and LAB topography is also a few tens of kilometres displaced towards the SE from the suture zone on the surface (Gîrbacea and Frisch, 1998; Mațenco, 2017). We propose that this feature and the elevated position of the Transylvanian Basin may be related to the same 'asthenospheric jamming' effect. This effect, however, is enhanced further by the thick European Platform on the E and the Moesian platform on the SE. These two thickened continental blocks force and focus the asthenospheric flow into the Carpathian Bend area, making its effect (i.e., active surface topography, intermediate depth earthquakes and gas emanations) more profound (e.g., Kovács et al., 2021). In line with this hypothesized SE directed asthenospheric push, the fast directions in the SE Carpathians show NE-SW direction (Ivan et al., 2008; Petrescu et al., 2020). This suggests that NE-SW oriented vertical foliation may develop in the root of the thick continental plates of Moesia and the stable European Platform perpendicular to the SE directed asthenospheric push.

Note that the effect of this "asthenospheric jam" in the Pannonian Basin may only be locally important, and have only a limited effect on the regional or continental-scale shear wave anisotropy pattern. These much larger-scale patterns may develop in response to regional-scale plate tectonic processes, including the overall mantle flow from the Alpine-Adriatic system towards the Hellenic Slab (e.g., Lo Bue et al., 2022), or the effect of the very thick European lithosphere on the east, which marks an important barrier for shallow asthenospheric flow trajectories with components towards the Trans European Suture zone (Qorbani et al., 2016). The observation that the overall delay times slightly increase towards the NE (i.e. the European platform) may imply the more profound effect of this thick lithospheric barrier. Future cross-European studies may shed further light on the horizontal and vertical variations of the anisotropy and its geodynamic implications.

5.4. Asthenospheric contribution to differential vertical movements

As pointed out in previous studies, lithospheric scale folding in the Pannonian Basin may be an important factor in generating late Neogene active differential vertical movements on the surface (Bada et al., 2007; Dombrádi et al., 2010). In addition, the recent Plio-Pleistocene uplift and erosion of the Transdanubian Central Range might be also related to

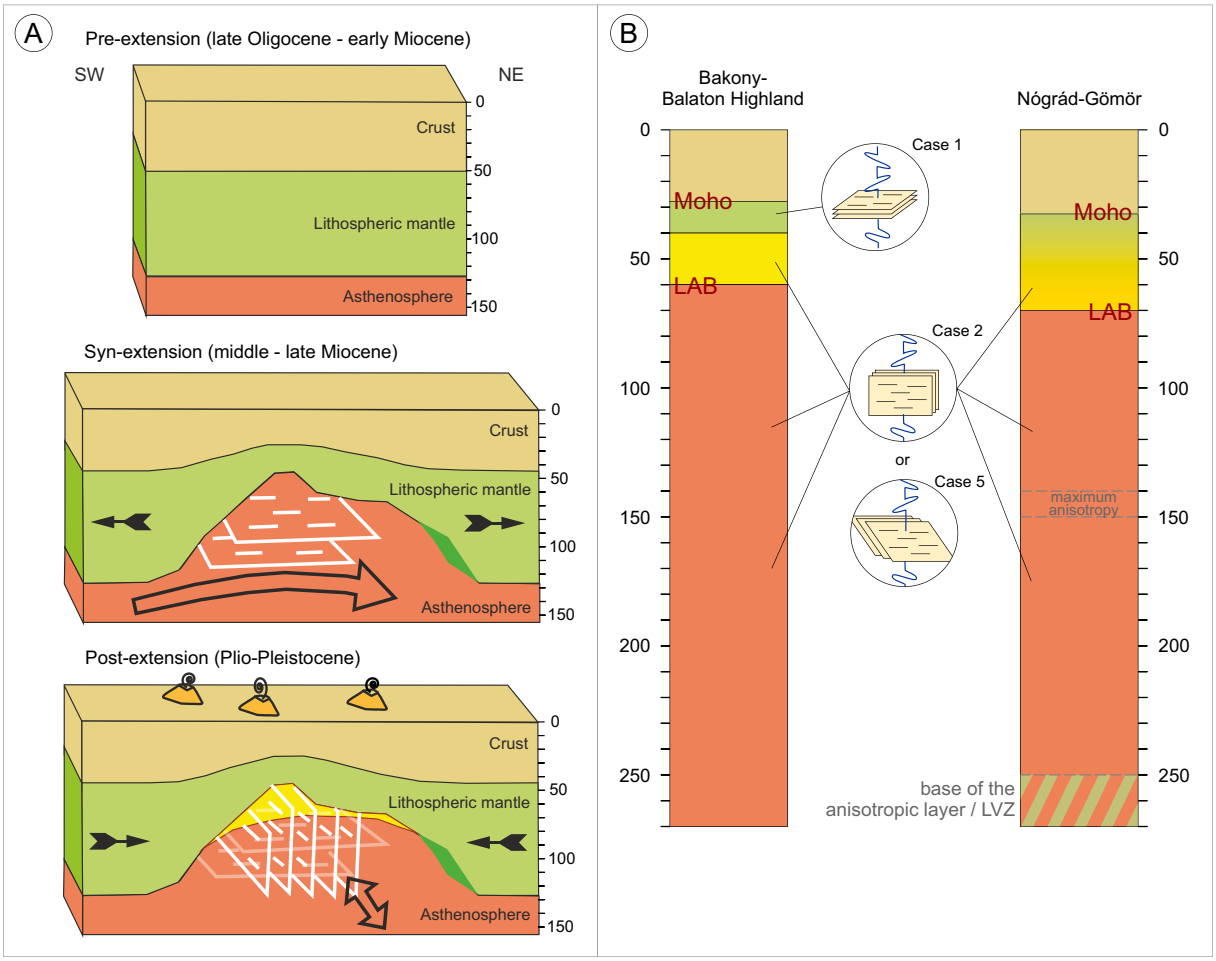

Fig. 13. A – Schematic illustration of the pre- *syn*- and post-extensional stage of the Pannonian Basin along a SW-NE section (see the location on Fig. 1). The assumed change of the orientation of the foliation and lineation in the asthenosphere during the syn- to post-extension stage is indicated as well, along with the directions of asthenospheric flow. B – Theoretical depth columns beneath the Bakony-Balaton Highland and Nógrád-Gömör volcanic fields with indications of the deformation structures and the major horizons. Approximate Moho and LAB depths are after Kalmár et al. (2021) and Tari et al. (1999), respectively.

this 'asthenospheric jam' beneath the Carpathian-Pannonian region.

According to geodetic measurements such as repeated precise levellings, the Transdanubian Range is the fastest rising area of the central and western part of the Pannonian Basin. However, Joó (1992) estimates the maximum uplift rate here slightly above 1 mm/year, whereas the maximum observed raw uplift rates are 0.5 mm/year in the Balaton Highland. As a result of GPS motion studies carried out since the early 1990s, an uplift rate of 0.3 mm/year is expected along the SW-NE axis of the Transdanubian Range (Grenerczy et al., 2005), which decreases rapidly away from the axis and changes into subsidence in the Great and Little Hungarian Plains.

For the present study it is not only the current uplift rate of the Transdanubian Range that is interesting, but also its evolution throughout the Neogene and Quaternary. Visnovitz et al. (2021) date the onset of structural inversion at Lake Balaton to about 8 million years ago from the seismically surveyed strata close to the Transdanubian central range. Ruszkiczay-Rüdiger et al., 2016; Ruszkiczay-Rüdiger et al., 2020) resolved key temporal changes in uplift rate, pointing to an important role of deep, asthenospheric driving forces. We propose that this 'asthenospheric jam' can be a viable contribution to the observed uplift. Why these vertical movements mainly affect the Transdanubian Central range remains an open question, but the notion that it has an increase in crustal thickness (~5 km; Kalmár et al., 2021). along its NE-SW oriented strike (i.e. perpendicular to the vertical foliation of the asthenosphere) may be an important factor as well as the vicinity of the also perpendicularly oriented Mid-Hungarian Zone.

6. Conclusions

Shear-wave splitting data and seismic properties of upper mantle xenoliths were jointly evaluated in the western part of the Carpathian-Pannonian region (CPR) to investigate the nature, depth extent and regional differences of mantle anisotropy in an extensional basin setting currently in a regime of tectonic inversion. Based on our results, anisotropy is different in the northern and in the central-southern part of the studied area.

In the northern part, beneath the Western Carpathians, the lack of azimuthal dependence of the fast S-component suggests a single anisotropic layer, with spatial coherency analyses putting the center at ~140–150 km, implying a total thickness of ~220–240 km. Calculated thicknesses from lattice preferred orientation of xenoliths from the Nógrád-Gömör volcanic field resulted in smaller values on average, which may be explained by slightly dipping instead of vertical foliation. Alternatively, xenoliths may not uniformly represent the anisotropic layer. In the central and western parts, systematic azimuthal variations point to multiple anisotropic layers. This can be linked to the two xenolith groups described from the Bakony-Balaton Highland, which represent a shallower, older lithospheric layer retaining syn-extension structural features, and a deeper, juvenile lithosphere which accreted during the post-extensional thermal relaxation. In the western part of

the Pannonian Basin, the remnant of a subducted slab from the Eurasian plate may account for the indication of multiple anisotropy.

The shear-wave splitting results along with previous observations in the CPR reveal a significant role of the asthenosphere not only in contributing to mantle anisotropy but also in deep seismic anomalies and surface topography as well. As a response to the tectonic inversion, the asthenosphere is vertically (or sub-vertically) foliated and forced to escape along the surrounding orogenic rim, perpendicular to the NE-SW compression. This asthenospheric flow could explain anomalous features such as displacement of Moho and LAB topographies in the SE margins of the CPR.

Supplementary data to this article can be found online at https://doi.org/10.1016/j.tecto.2022.229643.

Funding

This project was financially supported by the National Research, Development and Innovation Fund (Grant No. K141860, NN141956), the MTA FI Lendület Pannon LitH_2Oscope grant to I. J. Kovács, and the Distinguished Guest Scientist Fellowship Program of the Hungarian Academy of Sciences to S. Cloetingh.

CRediT authorship contribution statement

Nóra Liptai: Conceptualization, Writing – original draft, Visualization. **Zoltán Gráczer:** Software, Visualization, Data curation, Formal analysis, Writing - original draft. **Gyöngyvér Szanyi:** Software, Visualization, Data curation, Formal analysis, Writing - original draft. **Sierd A.P.L. Cloetingh:** Conceptualization, Writing – review & editing. **Bálint Süle:** Software, Data curation. **László E. Aradi:** Resources, Writing – review & editing. **György Falus:** Resources. **Götz Bokelmann:** Conceptualization, Writing – review & editing. **Máté Timkó:** Writing – review & editing. **Gábor Timár:** Writing – review & editing. **Csaba Szabó:** Resources. **István J. Kovács:** Conceptualization, Writing – original draft, Supervision, Funding acquisition.

Declaration of Competing Interest

The authors declare that they have no known competing financial interests or personal relationships that could have appeared to influence the work reported in this paper.

Data availability

Data will be made available on request.

Acknowledgements

The authors are indebted to Jaroslava Plomerová (Institute of Geophysics, Czech Academy of Sciences) for providing a gyrocompass for the sensor orientation measurements. We are grateful to all members of AlpArray Seismic Network Team: G. Hetényi, R. Abreu, I. Allegretti, M.-T. Apoloner, C. Aubert, S. Besançon, M. Bès De Berc, G. Bokelmann, D. Brunel, M. Capello, M. Čarman, A. Cavaliere, J. Chèze, C. Chiarabba, J. Clinton, G. Cougoulat, W. C. Crawford, L. Cristiano, T. Czifra, E. D'Alema, S. Danesi, R. Daniel, A. Dannowski, I. Dasović, A. Deschamps, J.-X. Dessa, C. Doubre, S. Egdorf, ETHZ-SED Electronics Lab, T. Fiket, K. Fischer, W. Friederich, F. Fuchs, S. Funke, D. Giardini, A. Govoni, Z. Gráczer, G. Gröschl, S. Heimers, B. Heit, D. Herak, M. Herak, J. Huber, D. Jarić, P. Jedlička, Y. Jia, H. Jund, E. Kissling, S. Klingen, B. Klotz, P. Kolínský, H. Kopp, M. Korn, J. Kotek, L. Kühne, K. Kuk, D. Lange, J. Loos, S. Lovati, D. Malengros, L. Margheriti, C. Maron, X. Martin, M. Massa, F. Mazzarini, T. Meier, L. Métral, I. Molinari, M. Moretti, A. Nardi, J. Pahor, A. Paul, C. Péquegnat, D. Petersen, D. Pesaresi, D. Piccinini, C. Piromallo, T. Plenefisch, J. Plomerová, S. Pondrelli, S. Prevolnik, R. Racine, M. Régnier, M. Reiss, J. Ritter, G. Rümpker, S. Salimbeni, M. Santulin, W. Scherer, S. Schippkus, D. Schulte-Kortnack, V. Šipka, S. Solarino, D. Spallarossa, K. Spieker, J. Stipčević, A. Strollo, B. Süle, G. Szanyi, E. Szűcs, C. Thomas, M. Thorwart, F. Tilmann, S. Ueding, M. Vallocchia, L. Vecsey, R. Voigt, J. Wassermann, Z. Wéber, C. Weidle, V. Wesztergom, G. Weyland, S. Wiemer, F. Wolf, D. Wolyniec, T. Zieke, M. Živčić, H. Žlebčíková.

We are grateful for the constructive comments and suggestions by two anonymous reviewers that significantly helped to improve the manuscript, and for the editorial handling by Claire Currie. We acknowledge the operation of the seismic networks used in this study: CR – Croatian Seismograph Network, University of Zagreb, Croatia; HU - Hungarian National Seismological Network (doi:10.14470/UH028726), CSFK GGI KRSZO, Hungary; SK - National Network of Seismic Stations of Slovakia (doi: 10.14470/FX099882), Earth Science Institute of the Slovak Academy of Sciences, Slovakia; Z3 – AlpArray Seismic Network (doi: 10.12686/ALPARRAY/Z3_2015), AlpArray Working Group; ZJ – PACASE Seismic Network (https://doi.org/10.7914/SN/ZJ_2019).

References

Aradi, L.E., Hidas, K., Kovács, I.J., Tommasi, A., Klébesz, R., Garrido, C.J., Szabó, C., 2017. Fluid-enhanced annealing in the subcontinental lithospheric mantle beneath the westernmost margin of the Carpathian-Pannonian extensional basin system. Tectonics 36, 2987–3011. https://doi.org/10.1002/2017TC004702.

Bada, G., Horváth, F., Dövényi, P., Szafián, P., Windhoffer, G., Cloetingh, S.A.P.L., 2007. Present-day stress field and tectonic inversion in the Pannonian basin. Glob. Planet. Chang. 58, 165–180. https://doi.org/10.1016/j.gloplacha.2007.01.007.

Baptiste, V., Tommasi, A., 2014. Petrophysical constraints on the seismic properties of the Kaapvaal craton mantle root. Solid Earth Discuss. 5 (2), 963–1005. https://doi.org/10.5194/sed-5-963-2013.

Baron, J., Morelli, A., 2017. Full-waveform seismic tomography of the Vrancea, Romania, subduction region. Phys. Earth Planet. Inter. 273, 36–49.

Barruol, G., Mainprice, D., 1993. A quantitative evaluation of the contribution of crustal rocks to the shear-wave splitting of teleseismic SKS waves. Phys. Earth Planet. Inter. 78 (3), 281–300. https://doi.org/10.1016/0031-9201(93)90161-2.

Bokelmann, G., Qorbani, E., Bianchi, I., 2013. Seismic anisotropy and large-scale deformation of the Eastern Alps. Earth Planet. Sci. Lett. 383, 1–6. https://doi.org/10.1016/j.epsl.2013.09.019.

Bus, Z., Grenerczy, G., Tóth, L., Mónus, P., 2009. Active crustal deformation in two seismogenic zones of the Pannonian region—GPS versus seismological observations. Tectonophysics 474 (1–2), 343–352.

Csontos, L., Vörös, A., 2004. Mesozoic plate tectonic reconstruction of the Carpathian region. Palaeogeogr. Palaeoclimatol. Palaeoecol. 210, 1–56. https://doi.org/10.1016/j.palaeo.2004.02.033.

Dando, B.D.E., Stuart, G.W., Houseman, G.A., Hegedűs, E., Brückl, E., Radovanović, S., 2011. Teleseismic tomography of the mantle in the Carpathian–Pannonian region of central Europe. Geophys. J. Int. 186, 11–31. https://doi.org/10.1111/j.1365-246X.2011.04998.x.

Dombrádi, E., Sokoutis, D., Bada, G., Cloetingh, S., Horváth, F., 2010. Modelling recent deformation of the Pannonian lithosphere: lithospheric folding and tectonic topography. Tectonophysics 484 (1–4), 103–118. https://doi.org/10.1016/j.tecto.2009.09.014.

Dricker, I., Vinnik, L., Roecker, S., Makeyeva, L., 1999. Upper-mantle flow in eastern Europe. Geophys. Res. Lett. 26, 1219–1222. https://doi.org/10.1029/1999GL900204.

Falus, G., 2004. Microstructural Analysis of Upper Mantle Peridotites: Their Application in Understanding Mantle Processes during the Formation of the Intra-Carpathian Basin System. Lithosphere Fluid Research Lab, Eötvös Loránd University, Budapest, p. 163.

Ferrand, T.P., Manea, E.F., 2021. Dehydration-induced earthquakes identified in a subducted oceanic slab beneath Vrancea, Romania. Sci. Rep. 11 (1), 1–9.

Gîrbacea, R., Frisch, W., 1998. Slab in the wrong place: lower lithospheric mantle delamination in the last stage of the Eastern Carpathian subduction retreat. Geology 26 (7), 611–614. https://doi.org/10.1130/0091-7613(1998)026<0611:SITWPL>2.3.CO;2.

Gráczer, Z., Szanyi, G., Bondár, I., Czanik, C., Czifra, T., Győri, E., Hetényi, G., Kovács, I., Molinari, I., Süle, B., Szűcs, E., Wesztergom, V., Wéber, Z., 2018. AlpArray in Hungary: temporary and permanent seismological networks in the transition zone between the Eastern Alps and the Pannonian basin. Acta Geod. Geophys. 221–245. https://doi.org/10.1007/s40328-018-0213-4.

Green, D.H., 2015. Experimental petrology of peridotites, including effects of water and carbon on melting in the Earth's upper mantle. Phys. Chem. Miner. 42, 95–122. https://doi.org/10.1007/s00269-014-0729-2.

Grenerczy, G., Sella, G., Stein, S., Kenyeres, A., 2005. Tectonic implications of the GPS velocity field in the northern Adriatic region. Geophys. Res. Lett. 32 https://doi.org/10.1029/2005GL022947. L16311.

Handy, M.R., Ustaszewski, K., Kissling, E., 2015. Reconstructing the Alps–Carpathians–Dinarides as a key to understanding switches in subduction polarity, slab gaps and surface motion. Int. J. Earth Sci. 104, 1–26. https://doi.org/10.1007/s00531-014-1060-3.

Hein, G., Kolinsky, P., Bianchi, I., Bokelmann, G., 2021. Shear-wave splitting in the Alpine region. Geophys. J. Int. 227, 1996–2015. https://doi.org/10.1093/gji/ggab305.

Hetényi, G., Molinari, I., Clinton, J., Bokelmann, G., Bondár, I., Crawford, W.C., Dessa, J.-X., Doubre, C., Friederich, W., Fuchs, F., Giardini, D., Gráczer, Z., Handy, M.R., Herak, M., Jia, Y., Kissling, E., Kopp, H., Korn, M., Margheriti, L., Meier, T., Mucciarelli, M., Paul, A., Pesaresi, D., Piromallo, C., Plenefisch, T., Plomerová, J., Ritter, J., Rümpker, G., Šipka, V., Spallarossa, D., Thomas, C., Tilmann, F., Wassermann, J., Weber, M., Wéber, Z., Wesztergom, V., Živčić, M., AlpArray Seismic Network Team, AlpArray OBS Cruise Crew, AlpArray Working Group, 2018. The AlpArray seismic network: a large-scale European experiment to image the Alpine orogen. Surv. Geophys. 39, 1009–1033. https://doi.org/10.1007/s10712-018-9472-4.

Hidas, K., Falus, G., Szabó, C., Szabó, P.J., Kovács, I., Földes, T., 2007. Geodynamic implications of flattened tabular equigranular textured peridotites from the Bakony-Balaton Highland Volcanic Field (Western Hungary). J. Geodyn. 43 (4–5), 484–503. https://doi.org/10.1016/j.jog.2006.10.007.

Horváth, F., 1993. Towards a mechanical model for the formation of the Pannonian basin. Tectonophysics 226, 333–357. https://doi.org/10.1016/0040-1951(93)90126-5.

Horváth, F., Cloetingh, S.A.P.L., 1996. Stress-induced late-stage subsidence anomalies in the Pannonian basin. Tectonophysics 266 (1–4), 287–300. https://doi.org/10.1016/S0040-1951(96)00194-1.

Horváth, F., Musitz, B., Balázs, A., Végh, A., Uhrin, A., Nádor, A., Koroknai, B., Pap, N., Tóth, T., Wórum, G., 2015. Evolution of the Pannonian basin and its geothermal resources. Geothermics 53, 328–352. https://doi.org/10.1016/j.geothermics.2014.07.009.

Houseman, G.A., Gemmer, L., 2007. Intra-orogenic extension driven by gravitational instability: Carpathian-Pannonian orogeny. Geology 35 (12), 1135–1138. https://doi.org/10.1130/G23993A.1.

Ivan, M., Popa, M., Ghica, D., 2008. SKS splitting observed at Romanian broad-band seismic network. Tectonophysics 462 (1–4), 89–98. https://doi.org/10.1016/j.tecto.2007.12.015.

Joó, I., 1992. Recent vertical surface movements in the Carpathian Basin. Tectonophysics 202 (2–4), 129–134. https://doi.org/10.1016/0040-1951(92)90091-J.

Jung, H., Katayama, I., Jiang, Z., Hiraga, T., Karato, S.I., 2006. Effect of water and stress on the lattice-preferred orientation of olivine. Tectonophysics 421 (1–2), 1–22. https://doi.org/10.1016/j.tecto.2006.02.011.

Kalmár, D., Hetényi, G., Balázs, A., Bondár, I., AlpArray Working Group, 2021. Crustal thinning from orogen to back-arc basin: the structure of the Pannonian Basin region revealed by P-to-S converted seismic waves. J. Geophys. Res. Solid Earth 126 (7). https://doi.org/10.1029/2020JB021309 e2020JB021309.

Klébesz, R., Gráczer, Z., Szanyi, G., Liptai, N., Kovács, I., Patkó, L., Pintér, Z., Falus, G., Wesztergom, V., Szabó, C., 2015. Constraints on the thickness and seismic properties of the lithosphere in an extensional setting (Nógrád-Gömör Volcanic Field, Northern Pannonian Basin). Acta Geod. Geophys. 50, 133–149. https://doi.org/10.1007/s40328-014-0094-0.

Kooi, H., Cloetingh, S., 1992. Lithospheric necking and regional isostasy at extensional basins 2. Stress-induced vertical motions and relative sea level changes. J. Geophys. Res. Solid Earth 97 (B12), 17573–17591. https://doi.org/10.1029/92JB01378.

Koulakov, I., Kaban, M.K., Tesauro, M., Cloetingh, S., 2009. P- and S-velocity anomalies in the upper mantle beneath Europe from tomographic inversion of ISC data. Geophys. J. Int. 179, 345–366. https://doi.org/10.1111/j.1365-246X.2009.04279.x.

Kovács, I., Csontos, L., Szabó, Cs, Bali, E., Falus, Gy, Benedek, K., Zajacz, Z., 2007. Paleogene–early miocene igneous rocks and geodynamics of the Alpine-Carpathian-Pannonian-Dinaric region: an integrated approach. In: Beccaluva, L., Bianchini, G., Wilson, M. (Eds.), Cenozoic Volcanism in the Mediterranean Area: Geological Society of America Special Paper, 418, pp. 93–112. https://doi.org/10.1130/2007.2418(05).

Kovács, I., Falus, G., Stuart, G., Hidas, K., Szabó, C., Flower, M., Hegedűs, E., Posgay, K., Zilahi-Sebess, L., 2012. Seismic anisotropy and deformation patterns in upper mantle xenoliths from the central Carpathian–Pannonian region: Asthenospheric flow as a driving force for Cenozoic extension and extrusion? Tectonophysics 514, 168–179. https://doi.org/10.1016/j.tecto.2011.10.022.

Kovács, I.J., Patkó, L., Liptai, N., Lange, T.P., Taracsák, Z., Cloetingh, S.A.P.L., Török, K., Király, E., Karátson, D., Biró, T., Kiss, J., Pálos, Z., Aradi, L.E., Falus, G., Hidas, K., Berkesi, M., Koptev, A., Novák, A., Wesztergom, V., Fancsik, T., Szabó, C., 2020. The role of water and compression in the genesis of alkaline basalts: inferences from the Carpathian-Pannonian region. Lithos 354-355. https://doi.org/10.1016/j.lithos.2019.105323, 105323.

Kovács, I.J., Liptai, N., Koptev, A., Cloetingh, S.A.P.L., Lange, T.P., Mațenco, L., Szakács, A., Radulian, M., Berkesi, M., Patkó, L., Molnár, G., Novák, A., Wesztergom, V., Szabó, C., Fancsik, T., 2021. The 'pargasosphere' hypothesis: looking at global plate tectonics from a new perspective. Glob. Planet. Chang. https://doi.org/10.1016/j.gloplacha.2021.103547, 103547.

Kreemer, C., Blewitt, G., Klein, E.C., 2014. A geodetic plate motion and Global Strain Rate Model. Geochem. Geophys. Geosyst. 15, 3849–3889. https://doi.org/10.1002/2014GC005407.

Latifi, K., Kaviani, A., Rümpker, G., Mahmoodabadi, M., Ghassemi, M.R., Sadidkhouy, A., 2018. The effect of crustal anisotropy on SKS splitting analysis—synthetic models and real-data observations. Geophys. J. Int. 213 (2), 1426–1447. https://doi.org/10.1093/gji/ggy053.

Lenkey, L., 1999. Geothermics of the Pannonian Basin and its Bearing on the Tectonics of Basin Evolution (PhD thesis). Vrije Universiteit, Amsterdam, The Netherlands.

Lippitsch, R., Kissling, E., Ansorge, J., 2003. Upper mantle structure beneath the Alpine orogen from high-resolution teleseismic tomography. J. Geophys. Res. Solid Earth 108. https://doi.org/10.1029/2002JB002016.

Liptai, N., Patkó, L., Kovács, I.J., Hidas, K., Pintér, Z., Jeffries, T., Zajacz, Z., O'Reilly, S.Y., Griffin, W.L., Pearson, N.J., Szabó, C., 2017. Multiple metasomatism beneath the Nógrád–Gömör Volcanic Field (Northern Pannonian Basin) revealed by upper mantle peridotite xenoliths. J. Petrol. 58 (6), 1107–1144. https://doi.org/10.1093/petrology/egx048.

Liptai, N., Hidas, K., Tommasi, A., Patkó, L., Kovács, I.J., Griffin, W.L., O'Reilly, S.Y., Pearson, N.J., Szabó, C., 2019. Lateral and vertical heterogeneity in the lithospheric mantle at the northern margin of the Pannonian Basin reconstructed from peridotite xenolith microstructures. J. Geophys. Res. Solid Earth 124, 6315–6336. https://doi.org/10.1029/2018JB016582.

Liptai, N., Lange, T.P., Patkó, L., Pintér, Z., Berkesi, M., Aradi, L.E., Szabó, C., Kovács, I.J., 2021. Effect of water on the rheology of the lithospheric mantle in young extensional basin systems as shown by xenoliths from the Carpathian-Pannonian region. Glob. Planet. Chang. 196, 103364 https://doi.org/10.1016/j.gloplacha.2020.103364.

Liu, K.H., Gao, S.S., 2011. Estimation of the depth of anisotropy using spatial coherency of shear-wave splitting parameters. Bull. Seismol. Soc. Am. 101, 2153–2161. https://doi.org/10.1785/0120100258.

Liu, K.H., Gao, S.S., 2013. Making reliable shear-wave splitting measurements. Bull. Seismol. Soc. Am. 103, 2680–2693. https://doi.org/10.1785/0120120355.

Lo Bue, R., Rappisi, F., Vanderbeek, B.P., Faccenda, M., 2022. Tomographic image Interpretation and Central-Western Mediterranean-like upper mantle dynamics from coupled seismological and geodynamic modeling approach. Front. Earth Sci. 10 https://doi.org/10.3389/feart.2022.884100, 884100.

Löberich, E., Long, M.D., Wagner, L.S., Qorbani, E., Bokelmann, G., 2021. Constraints on olivine deformation from SKS shear-wave splitting beneath the Southern Cascadia subduction zone back-arc. Geochem. Geophys. Geosyst. 22 (11) https://doi.org/10.1029/2021GC010091 e2021GC010091.

Mainprice, D., 1990. A FORTRAN program to calculate seismic anisotropy from the lattice preferred orientation of minerals. Comput. Geosci. 16, 385–393. https://doi.org/10.1016/0098-3004(90)90072-2.

Martin, M.J.R.R., Ritter, J.R.R., CALIXTO Working Group, 2005. High-resolution teleseismic body-wave tomography beneath SE Romania—I. Implications for three-dimensional versus one-dimensional crustal correction strategies with a new crustal velocity model. Geophys. J. Int. 162 (2), 448–460.

Mațenco, L., 2017. Tectonics and exhumation of Romanian Carpathians: Inferences from kinematic and thermochronological studies. In: Radoane, M., Vespremeanu-Stroe, A. (Eds.), Landform Dynamics and Evolution in Romania. Springer Geography. Springer, Cham. https://doi.org/10.1007/978-3-319-32589-7_2.

Mitterbauer, U., Behm, M., Brückl, E., Lippitsch, R., Guterch, A., Keller, G.R., Koslovskaya, E., Rumpfhuber, E.-M., Šumanovac, F., 2011. Shape and origin of the East-Alpine slab constrained by the ALPASS teleseismic model. Tectonophysics 510, 195–206. https://doi.org/10.1016/j.tecto.2011.07.001.

Patkó, L., Liptai, N., Kovács, I.J., Aradi, L.E., Xia, Q.-K., Ingrin, J., Mihály, J., O'Reilly, S.Y., Griffin, W.L., Wesztergom, V., Szabó, C., 2019. Extremely low structural hydroxyl contents in upper mantle xenoliths from the Nógrád-Gömör Volcanic Field (northern Pannonian Basin): Geodynamic implications and the role of post-eruptive re-equilibration. Chem. Geol. 507, 23–41. https://doi.org/10.1016/j.chemgeo.2018.12.017.

Patkó, L., Novák, A., Klébesz, R., Liptai, N., Lange, T.P., Molnár, G., Csontos, L., Wesztergom, V., Kovács, I.J., Szabó, C., 2021. Effect of metasomatism on the electrical resistivity of the lithospheric mantle – an integrated research using magnetotelluric sounding and xenoliths beneath the Nógrád-Gömör Volcanic Field. Glob. Planet. Chang. 197, 103389. https://doi.org/10.1016/j.gloplacha.2020.103389.

Paul, A., Karabulut, H., Mutlu, A.K., Salaün, G., 2014. A comprehensive and densely sampled map of shear-wave azimuthal anisotropy in the Aegean–Anatolia region. Earth Planet. Sci. Lett. 389, 14–22. https://doi.org/10.1016/j.epsl.2013.12.019.

Pécskay, Z., Lexa, J., Balogh, K., Seghedi, I., Konečny, V., Kovács, M., Márton, E., Kaliciak, M., Széky-Fux, V., Póka, T., Gyarmati, P., Edelstein, O., Rosu, E., Zec, B., 1995. Space and time distribution of Neogene-Quartenary volcanism in the Carpatho-Pannonian Region. Acta Vulcanol. 7, 15–28.

Pera, E., Mainprice, D., Burlini, L., 2003. Anisotropic seismic properties of the upper mantle beneath the Torre Alfina area (Northern Apennines, Central Italy). Tectonophysics 370, 11–30. https://doi.org/10.1016/S0040-1951(03)00175-6.

Petrescu, L., Stuart, G., Houseman, G., Bastow, I., 2020. Upper mantle deformation signatures of craton–orogen interaction in the Carpathian–Pannonian region from SKS anisotropy analysis. Geophys. J. Int. 220, 2105–2118. https://doi.org/10.1093/gji/ggz573.

Plomerová, J., Šílený, J., Babuška, V., 1996. Joint interpretation of upper-mantle anisotropy based on teleseismic P-travel time delays and inversion of shear-wave splitting parameters. Phys. Earth Planet. Inter. 95 (3–4), 293–309.

Plomerová, J., Achauer, U., Babuška, V., Vecsey, L., BOHEMA Working Group, 2007. Upper mantle beneath the Eger Rift (Central Europe): plume or asthenosphere upwelling? Geophys. J. Int. 169 (2), 675–682.

Plomerová, J., Vecsey, L., Babuška, V., 2012. Mapping seismic anisotropy of the lithospheric mantle beneath the northern and eastern Bohemian Massif (Central Europe). Tectonophysics 564, 38–53. https://doi.org/10.1016/j.tecto.2011.08.011.

Qorbani, E., Bianchi, I., Bokelmann, G., 2015. Slab detachment under the Eastern Alps seen by seismic anisotropy. Earth Planet. Sci. Lett. 409, 96–108. https://doi.org/10.1016/j.epsl.2014.10.049.

Qorbani, E., Bokelmann, G., Kovács, I., Horváth, F., Falus, G., 2016. Deformation in the asthenospheric mantle beneath the Carpathian-Pannonian Region. J. Geophys. Res. Solid Earth 121, 6644–6657. https://doi.org/10.1002/2015JB012604.

Ratschbacher, L., Merle, O., Davy, P., Cobbold, P., 1991. Lateral extrusion in the Eastern Alps, part 1: boundary conditions and experiments scaled for gravity. Tectonics 10, 245–256. https://doi.org/10.1029/90TC02622.

Ren, Y., Stuart, G.W., Houseman, G.A., Dando, B., Ionescu, C., Hegedűs, E., Radovanović, S., Shen, Y., 2012. Upper mantle structures beneath the Carpathian–Pannonian region: implications for the geodynamics of continental collision. Earth Planet. Sci. Lett. 349, 139–152. https://doi.org/10.1016/j.epsl.2012.06.037.

Royden, L.H., Horvath, F., Burchfiel, B.C., 1982. Transform faulting, extension, and subduction in the Carpathian Pannonian region. Geol. Soc. Am. Bull. 93, 717–725, 10.1130/0016-7606(1982)93<717:TFEASI>2.0.CO;2.

Royden, L., Horváth, F., Nagymarosy, A., Stegena, L., 1983. Evolution of the Pannonian basin system: . subsidence and thermal history2. Tectonics 2 (1), 91–137. https://doi.org/10.1029/TC002i001p00091.

Ruszkiczay-Rüdiger, Z., Braucher, R., Novothny, Á., Csillag, G., Fodor, L., Molnár, G., Madarász, B., ASTER Team, 2016. Tectonic and climatic forcing on terrace formation: coupling in situ produced 10Be depth profiles and luminescence approach, Danube River, Hungary, Central Europe. Quat. Sci. Rev. 131, 127–147. https://doi.org/10.1016/j.quascirev.2015.10.041.

Ruszkiczay-Rüdiger, Z., Balázs, A., Csillag, G., Drijkoningen, G., Fodor, L., 2020. Uplift of the Transdanubian Range, Pannonian Basin: how fast and why? Glob. Planet. Chang. 192, 103263 https://doi.org/10.1016/j.gloplacha.2020.103263.

Schmid, S.M., Bernoulli, D., Fügenschuh, B., Matenco, L., Schefer, S., Schuster, R., Tischler, M., Ustaszewski, K., 2008. The Alpine-Carpathian-Dinaridic orogenic system: correlation and evolution of tectonic units. Swiss J. Geosci. 101, 139–183. https://doi.org/10.1007/s00015-008-1247-3.

Seghedi, I., Downes, H., Szakács, A., Mason, P.R., Thirlwall, M.F., Roşu, E., Pécskay, Z., Márton, E., Panaiotu, C., 2004. Neogene–Quaternary magmatism and geodynamics in the Carpathian–Pannonian region: a synthesis. Lithos 72 (3–4), 117–146. https://doi.org/10.1016/j.lithos.2003.08.006.

Silver, P.G., 1996. Seismic anisotropy beneath the continents: probing the depths of geology. Annu. Rev. Earth Planet. Sci. 24, 385–432. https://doi.org/10.1146/annurev.earth.24.1.385.

Silver, P.G., Chan, W.W., 1991. Shear wave splitting and subcontinental mantle deformation. J. Geophys. Res. Solid Earth 96, 16429–16454. https://doi.org/10.1029/91JB00899.

Silver, P.G., Savage, M.K., 1994. The interpretation of shear-wave splitting parameters in the presence of two anisotropic layers. Geophys. J. Int. 119, 949–963. https://doi.org/10.1111/j.1365-246X.1994.tb04027.x.

Song, W., Yu, Y., Shen, C., Lu, F., Kong, F., 2019. Asthenospheric flow beneath the Carpathian-Pannonian Region: constraints from shear wave splitting analysis. Earth Planet. Sci. Lett. 520, 231–240. https://doi.org/10.1016/j.epsl.2019.05.045.

Szabó, C., Harangi, S., Csontos, L., 1992. Review of Neogene and Quaternary volcanism of the Carpathian-Pannonian region. Tectonophysics 208 (1–3), 243–256. https://doi.org/10.1016/0040-1951(92)90347-9.

Szabó, C., Falus, G., Zajacz, Z., Kovács, I., Bali, E., 2004. Composition and evolution of lithosphere beneath the Carpathian–Pannonian Region: a review. Tectonophysics 393, 119–137. https://doi.org/10.1016/j.tecto.2004.07.031.

Tari, G., Dövényi, P., Dunkl, I., Horváth, F., Lenkey, L., Stefanescu, M., Szafián, P., Tóth, T., 1999. Lithospheric structure of the Pannonian basin derived from seismic, gravity and geothermal data. Geol. Soc. Lond., Spec. Publ. 156 (1), 215–250. https://doi.org/10.1144/GSL.SP.1999.156.01.12.

Tari, G., Horváth, F., 2010. Eo-Alpine evolution of the Transdanubian Range in the nappe system of the Eastern Alps: revival of a 15 years old tectonic model. Bulletin of the Hungarian Geological Society (in Hungarian with English abstract) 140, 483–510.

Tašárová, A., Afonso, J.C., Bielik, M., Götze, H.J., Hók, J., 2009. The lithospheric structure of the Western Carpathian–Pannonian Basin region based on the CELEBRATION 2000 seismic experiment and gravity modelling. Tectonophysics 475 (3–4), 454–469. https://doi.org/10.1016/j.tecto.2009.06.003.

Thybo, H., 2006. The heterogeneous upper mantle low velocity zone. Tectonophysics 416 (1–4), 53–79. https://doi.org/10.1016/j.tecto.2005.11.021.

Timkó, M., Kovács, I., Wéber, Z., 2019. 3D P-wave velocity image beneath the Pannonian Basin using traveltime tomography. Acta Geod. Geophys. 54 (3), 373–386. https://doi.org/10.1007/s40328-019-00267-3.

Tommasi, A., Vauchez, A., 2015. Heterogeneity and anisotropy in the lithospheric mantle. Tectonophysics 661, 11–37.

van Gelder, I.E., Willingshofer, E., Sokoutis, D., Cloetingh, S.A.P.L., 2017. The interplay between subduction and lateral extrusion: a case study for the European Eastern Alps based on analogue models. Earth Planet. Sci. Lett. 472, 82–94. https://doi.org/10.1016/j.epsl.2017.05.012.

Visnovitz, F., Jakab, B., Czecze, B., Hámori, Z., Székely, B., Fodor, L., Horváth, F., 2021. High resolution architecture of neotectonic fault zones and post-8-Ma deformations in western Hungary: Observations and neotectonic characteristics of the fault zone at the Eastern Lake Balaton. Global and Planetary Change 203, 103540. https://doi.org/10.1016/j.gloplacha.2021.103540.

Wortel, M.J.R., Spakman, W., 2000. Subduction and slab detachment in the Mediterranean-Carpathian Region. Science 290, 1910–1917. https://doi.org/10.1126/science.290.5498.1910.

Wüstefeld, A., Bokelmann, G., Zaroli, C., Barruol, G., 2008. SplitLab: a shear-wave splitting environment in Matlab. Comput. Geosci. 34, 515–528. https://doi.org/10.1016/j.cageo.2007.08.002.

Yang, B.B., Gao, S.S., Liu, K.H., Elsheikh, A.A., Lemnifi, A.A., Refayee, H.A., Yu, Y., 2014. Seismic anisotropy and mantle flow beneath the northern Great Plains of North America. J. Geophys. Res. Solid Earth 119, 1971–1985. https://doi.org/10.1002/2013JB010561.

Zhu, H., Tromp, J., 2013. Mapping tectonic deformation in the crust and upper mantle beneath Europe and the North Atlantic Ocean. Science 341, 871–875. https://doi.org/10.1126/science.1241335.